Digital Control of a VCO for Radar Applications

Master's Thesis in Control Theory and Embedded System Design

Lund University
Faculty of Engineering, LTH

Department of Automatic Control

LUND
UNIVERSITY

Authors: Martin Alumets & Mattias Evaldsson
Industrial Supervisors: Lars Andersson & Andreas Glatz
Academic Supervisor: Anton Cervin
Examiner: Kristian Soltesz

29th August 2021

MSc Thesis
TFRT-6148
ISSN 0280-5316

Department of Automatic Control
Lund University
Box 118
SE-221 00 LUND
Sweden

Printed in Sweden by Tryckeriet i E-huset
Lund 2021

Abstract

Radar systems have been around since the early 20th century, and technology is advancing at an ever-increasing speed. This has led to great achievements in radar development, which have expanded the technology's area of use. One of these is the application of a security radar used in conjunction with security cameras for increased flexibility and reliability in security systems. A type of radar that is suited for security applications is the frequency modulated continuous wave radar, and it requires a control system to stay within the allocated radar frequency spectrum and to increase the radar's performance. This control system is often implemented with analogue components, which comes with extra costs and space requirements. This master thesis aims to investigate a digital control method and analyse the performance of it. This comes with the advantage of not requiring any extra components for the control system and rely on the micro control unit used to analyse the radar data.

Acknowledgements

We would like to extend our gratitude to all of our supervisors, who helped us during the Master Thesis. Firstly, to our industrial supervisors at AXIS, Lars Andersson and Andreas Glatz, who have supported us with their knowledge in radar technology and embedded electronics throughout the project. Secondly to our academic supervisor Anton Cervin, from the Department of Automatic Control of LTH, for helping us with the control part of the thesis and giving us a lot of constructive feedback on the report. Finally, we would like to thank Axis for letting us do our Master Thesis for them.

Notations and Symbols

PIR - Passive Infrared Sensor
FMCW - Frequency Modulated Continuous Wave
VCO - Voltage Controlled Oscillator
PLL - Phase Locked Loop
MCU - Microcontroller Unit
RADAR - Radio Aim Detection And Ranging
FFT - Fast Fourier Transform
AoA - Angle of Arrival
ADC - Analogue to Digital Conversion
I - In phase
Q - Quadrature
RX - Receive
TX - Transmit
PID - Proportional Integral Derivative
PCB - Printed Circuit Board
DAC - Digital to Analogue Conversion
DSP - Digital Signal Processing
EMI - Electromagnetic Interference
IF - Intermediate Frequency
RC filter - Resistor–Capacitor filter
FILO - First In Last Out
RAM - Random Access Memory

Contents

1 Introduction

Radar technology has developed a lot during the last years, and a result of that has been smaller and cheaper radar modules[1]. The new technology has lead to a lot of new areas of use, involving detection sensors for example in the automotive industry. However, recently it has also been shown to be usable in the security sector, where Axis has started to utilise the technology[2].

In the security business, small radars could either be used as movement triggers for security cameras or lights. It could also be used as a complement to the passive infrared sensor (PIR) sensor that is often used for these applications. PIR operates on temperature change, which has some disadvantages when operating in hot environments and when there are particles in the air [3]. The sensor can not distinguish human movement in environments where the temperature is close to 37 degrees Celsius as could be the case in some countries. Also, sometimes false alarms are triggered from different light sources, as tail lights and exposure to sunlight. As radars can operate in any environment and also can be used to calculate distance, velocity and direction, it has an advantage for this use case in comparison to a PIR sensor.

There are several types of radars, and a common type is the Frequency-Modulated Continuous-Wave (FMCW) type. The FMCW radar uses a frequency-modulated signal to sweep a frequency range. To do this a Voltage-Controlled Oscillator (VCO) can be used. The VCO is used to convert a voltage to a sinusoidal signal with a very high frequency. But due to the VCOs temperature dependency and non-linear conversion from voltage to frequency, it requires some control system to work in a broad temperature range and have high accuracy. This control system is often implemented with a Phase-Locked Loop (PLL), which is an analogue control method.

Purpose

The objective of this Master Thesis is to investigate the possibility to digitally control a VCO without using a PLL. The reason for this is to lower component costs, by only using an MCU with no additional components. The result of achieving this without a PLL would be a cheaper and space-efficient product. This is especially important for a small radar that could rival a PIR in price while still having the advantages that come with radar.

Problem Formulation

The following are the main objectives of the thesis:

- Investigate different solutions for digital control of a voltage controlled oscillator.
- Implement the most suitable solution on a microcontroller and evaluate its performance.
- Evaluate the requirements of the hardware for a working radar product.

Methodology

First, the problems that had to be solved were identified and different solutions for the problems were researched. The most promising solutions were then verified by simulations in different computer software. Finally, the solutions were implemented on a prototype and the prototype's performance was evaluated.

Outline

Chapter 2 includes a background to radar theory, a description of the VCO´s behaviour and theory of commonly used control methods.

Chapter 3 consists of a description of the system layout, the implementation of the control method used for linearizing the VCO and the test conducted to evaluate the results of the implementation.

Chapter 4 presents all results and analysis of them. Also future work suggestions are gives in this section.

Chapter 5 summarises the Master Thesis and the most important information form the previous chapters.

2 Background

This chapter gives an introduction to the background, the theory and general concepts of radars. This, involves the history of radars, frequency bands and multiple formulas for describing different aspects of radar theory. Furthermore, the characteristics of the VCO is presented, as well as different control methods.

2.1 Radar Theory

2.1.1 Radar History

Radio Aim Detection And Ranging, or radar, was first used in the military during the 1930s. However, the history of it started even earlier, with the discovery of electromagnetic fields during the 1880s. The German physicist Heinrich Hertz conducted experiments verifying the fundamental laws of electromagnetic fields, that stated that both light and radio are electromagnetic waves, however with different frequency. These laws had earlier been formulated theoretically by the Scottish physicist James Clerk Maxwell. The verification of these laws became the start of research for radars, however it was not until the end of the 1930s the technology was first used in practice. The British physicist Sir Robert Watson-Watt developed a 30MHz radar that was used during World War II to support British air force defence against the Germans. Other countries also deployed radars during the same time, however the British is considered to be the first[4].

In present time, radars are utilised in multiple areas, including detection of spacecraft, aircraft, ships at sea, however also insects and birds in the atmosphere. Furthermore, radars are used to measure speeds of vehicles, measure different attributes of oceans, map the surface of the earth and determine weather behaviours[5]. As the use of radars has become more widely spread in different areas they have also become cheaper, resulting in additional applications[1] being developed.

Radars operate in a wide electromagnetic spectrum. The different frequencies have to do with the area of usage for the radar. Lower frequencies are used for applications that require long range and higher frequencies are used for shorter ranges with higher precision. Frequency bands that are commonly used in industries are C-band, X-band, K-band, and W-band [6]. The C-band ranges between 4-8 GHz and is used for satellite communication, satellite-TV, weather radars and for the 5GHz part of Wi-Fi communication[7]. The X-band has a frequency range of 8-12 GHz and is used for radar applications including air traffic management, waterborne traffic control, weather monitoring, vehicle detection, and defence tracking[8]. The K-band operates between 18-27 GHz and includes applications as short range and high resolution radar as well as satellite communications and astronomical observations[9]. The W-band

operates at higher frequencies between 75-110 GHz, and is established in a variate of areas including defence, different security applications, satellite communication and automotive radars[10].

Other then the bands mentioned above there are also the ISM bands (industrial, scientific or medical frequency bands). The bands are commonly used for radar equipment and have the upside that they are free from regulations. The bands could have small variations in different countries, the US ISM band can be seen in Figure 2.1 [11].

Frequency	Frequency Range	Bandwidth	Thereof license free(*1)	License free bandwidth(*1)
24 GHz	24.00 - 24.25 GHz	0.25 GHz	24.15 - 24.25 GHz	0.10 GHz
61 GHz	61.00 - 61.50 GHz	0.50 GHz	61.00 - 61.50 GHz	0.50 GHz
122 GHz	122.00 - 123.00 GHz(*2)	1.00 GHz	122.25 - 123.00 GHz	0.75 GHz
244 GHz	244.00 - 246.00 GHz	2.00 GHz	244.00 - 246.00 GHz	2.00 GHz

Figure 2.1: The US ISM bands. [11]

2.1.2 The Radar Principle

The radar principle is based on a transmitter sending out multiple electromagnetic pulses. The pulses travel from the antenna through the medium it is operating in, until reflected on an object or surface. When reflected, some of the waves travel back to a receiver, and the time it takes is also known as round trip time. The receiver is either the same antenna as the transmitting one, or a separate placed close to the transmitter. By calculating the time between the transmitted signal and the reflected signal, the distance to the reflecting object can be calculated. This type of radar is called "pulse radar" and is illustrated in Figure 2.2.[6]

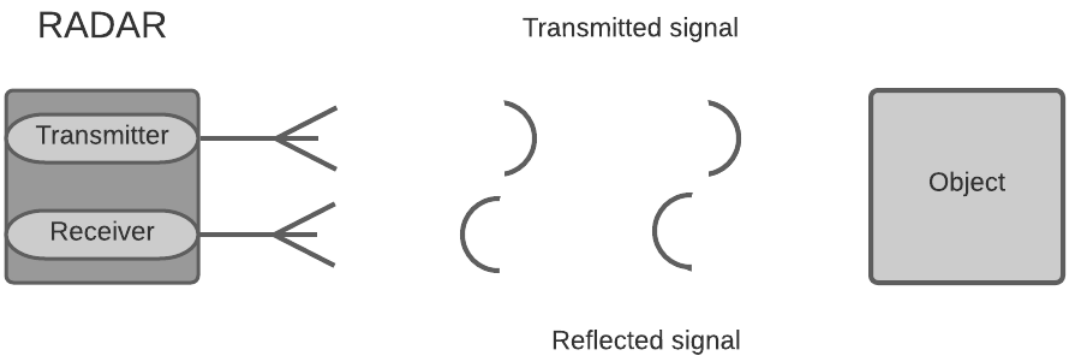

Figure 2.2: Illustration of how a pulse radar works.

The fundamental behaviour and limitations of radars can be expressed by two equations, "the radar equation" and "the range equation". The radar equation describes the proportion between the transmitted and the received power and is expressed as follows [12]:

$$\frac{P_r}{P_t} = \frac{g_t \cdot g_r \cdot \sigma}{R^4}, \tag{2.1}$$

where P_t is the transmitted power, P_r is the received power, g_t is the antenna gain of the transmitted signal, g_r is the antenna gain of the received signal, σ is the radar cross-section and R is the distance to the object from the radar. [12] An illustrative picture of this can be seen in Figure 2.3.

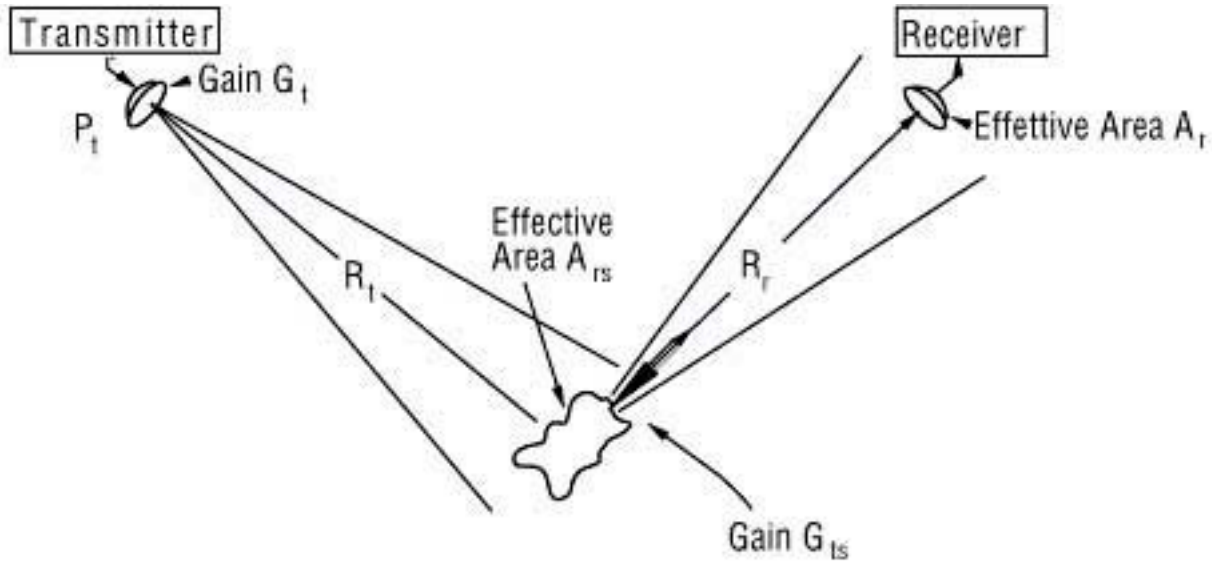

Figure 2.3: Radar Equation Principle [13]

.

The antenna gain depends on the size of the effective area of the antenna and the efficiency of it[14]. The range equation describes the maximum range in correlation to power dissipation and it is derived from the radar equation and can be seen in Equation 2.2.

$$R = \sqrt[4]{\frac{P_t \cdot g_t \cdot g_r \cdot \sigma}{P_r}} \tag{2.2}$$

From Equation 2.2 it can be seen that the range depends on the transmitted power of the signal, transmitter and the receivers gain and the area of the object divided by the received power of the antenna.

2.1.3 FMCW - Frequency Modulated Continuous Wave

Due to the difficulty in measuring a short round trip time to an object with radar signals, a technology called Frequency Modulated Continuous Wave (FMCW) is often used for short range radars. The frequency modulated signal, or "chirp" is used to measure the change in frequency between the transmitted and the received signal. This signal, called the beat frequency or IF-signal, is produced by mixing the outgoing and incoming signal as illustrated in Figure 2.4. The beat frequency is directly correlated to the distance of the target, but to measure the velocity and angle to a target several chirps have to be sent in quick succession and with more then one receiving antenna. [12]

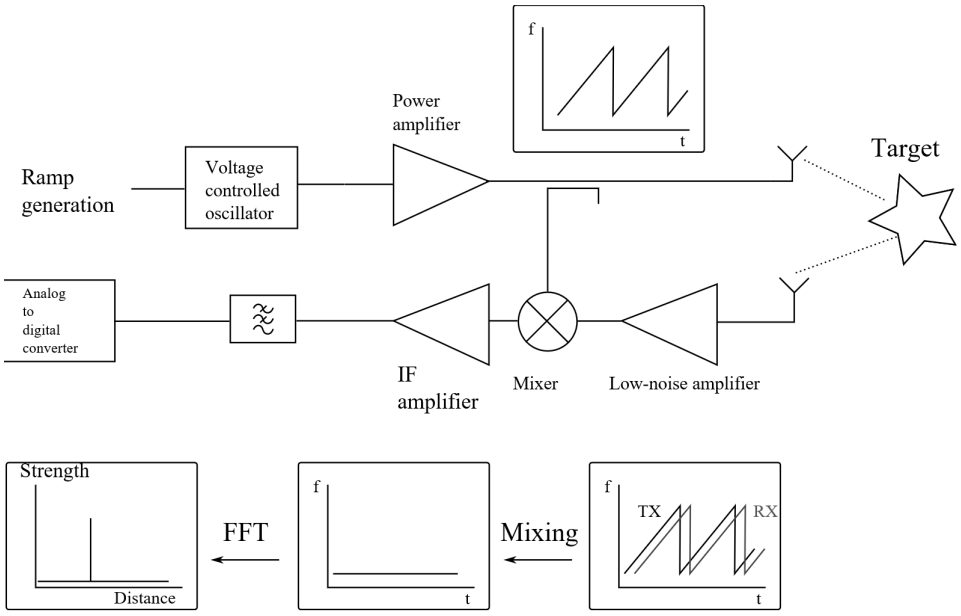

Figure 2.4: FMCW Principle. [15]

Range

To calculate the distance to a target the frequency of the sent signal is compared with the frequency of the received signal and with the use of Equation 2.3 the distance can be calculated. The major advantage of this method for calculating the range is the avoidance of measuring the round trip time which is in the order of nanoseconds for targets in the range of a few meters. Instead only the beat frequency has to be measured to calculate the range, see Equation 2.5. This is done by performing a Fast Fourier Transform (FFT) on the measured signal and each peak of the spectrum will correspond to a target of the radar.[16]

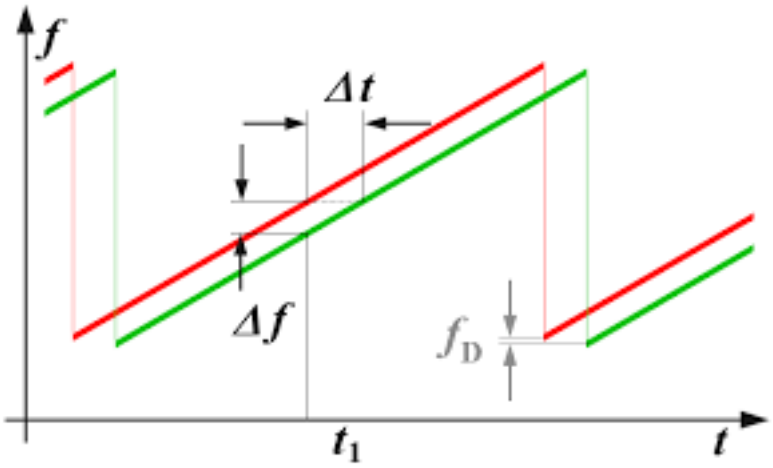

Figure 2.5: FMCW with Sawtooth Frequency Modulation. The red line is the sent chirp and the green is the received signal.[17]

$$R = \frac{c_0 \cdot |\Delta t|}{2} = \frac{c_0 \cdot |\Delta f|}{2\frac{\mathrm{d}f}{\mathrm{d}t}}, \tag{2.3}$$

where R is the range to the object, Δt is the round trip time, Δf is the beat frequency, $\frac{\mathrm{d}f}{\mathrm{d}t} = \frac{f_{BW}}{T_c}$ is the slope of the chirp, c_0 is the speed of light, T_c is the time of a chirp and f_{BW} is the bandwidth.

The range resolution of the FMCW type of radar can be viewed as the lowest distance between two targets that can be distinguished in the FFT spectrum of the beat frequency and it is dependant on the bandwidth of the chirp. This is illustrated in Figure 2.6,where on the right side two targets are at a range too similar to be able to separate them in the FFT spectrum. The range resolution is not a factor that can easily be changed due to the radio spectrum regulations that decide the allowed frequency range and the full span of the allocated bandwidth is therefore used to maximise the range resolution. [18]

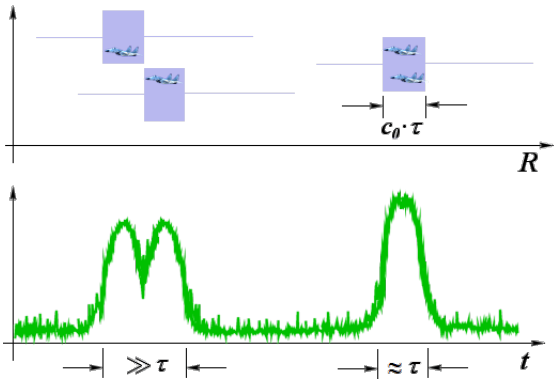

Figure 2.6: Minimum distance between two objects to be distinguished and not. To the left two objects can be separated in range and to the right they can not [19].

The range resolution can be calculated with Equation 2.4, this can also be formulated as Equation 2.5 which can be used to calculate the lowest change in the FFT spectrum that can be separated as two different objects. [19]

$$R_{res} = \frac{c_0}{2T_c \frac{\mathrm{d}f}{\mathrm{d}t}} = \frac{c_0}{2B} \tag{2.4}$$

$$\Delta f_{FTT} = \frac{\frac{\mathrm{d}f}{\mathrm{d}t}}{f_{BW}} = \frac{1}{T_c}, \tag{2.5}$$

where R_{Res} is the lowest change in range and Δf_{FTT} is the lowest change in beat frequency.

The theoretical maximum range of the radar is calculated with Equation 2.6 and this is dependant on how high beat frequency can be measured as the sampling frequency for the FFT has to be higher than the beat frequency to ensure no aliasing. [18]

$$R_{max} = \frac{f_s c_0}{2\frac{\mathrm{d}f}{\mathrm{d}t}}, \tag{2.6}$$

where R_{max} is the maximum range and f_s is the sampling frequency.

Velocity

The velocity of a target can be calculated by comparing the phase shift between the beat frequency from several chirps. The phase shift is sensitive to the range differential which can be seen in Equation 2.7. This formula describes the relation between the phase shift and the range differential which in turn can be used to calculate the velocity.[20]

$$\Delta\Phi = 2\pi f_c \Delta\tau = \frac{2\pi\Delta R}{\lambda}, \tag{2.7}$$

where $\Delta\Phi$ is the phase shift between two chirps, f_c is the chirps carrier frequency, ΔR is the range difference to the object for two chirps and λ is the wavelength

By transmitting multiple chirps separated by the chirp time T_c and measuring the phase shift between the chirps the target velocity can be calculated with Equation 2.8. The phase shift is calculated with Doppler FFT.[20]

$$v = \frac{\lambda\Delta\Phi}{4\pi T_c}, \tag{2.8}$$

where v is the velocity of the moving object.

The velocity resolution v_{res} is the minimum separation between two targets velocity for them to be shown as two different peaks in the Doppler-FFT. The formula for calculating the velocity resolution is seen in Equation 2.9. [20]

$$\begin{aligned} \Delta\Phi &> \frac{2\Phi}{N} \\ v &> \frac{\lambda}{2NT_c} \\ \Rightarrow v_{res} &= \frac{\lambda}{2T_f}, \end{aligned} \tag{2.9}$$

where N is the number of chirps and T_f is the time of one frame.

The maximum measurable velocity v_{max} can be calculated with formula 2.10. This is because it is impossible to know if the phase has moved clockwise or counter-clockwise if the phase shift is larger than ϕ radians and this has to be known to derive the movement direction of the target. [20]

$$\begin{aligned} \Delta\Phi &< \pi \\ v &< \frac{\lambda}{4T_c} \\ \Rightarrow v_{max} &= \frac{\lambda}{4T_c}, \end{aligned} \tag{2.10}$$

FFT over Frames

The sent chirps are often compiled in sets that are called frames, the frame is a matrix of measured values for each corresponding chirp. To increase the signal strength both the range FFT and the Doppler FFT is done over the whole frame and the result can then be combined to differentiate disturbance compared to a real target. Figure 2.7 shows how this is done first by calculating the range over the columns and then over the rows for the velocity. [21]

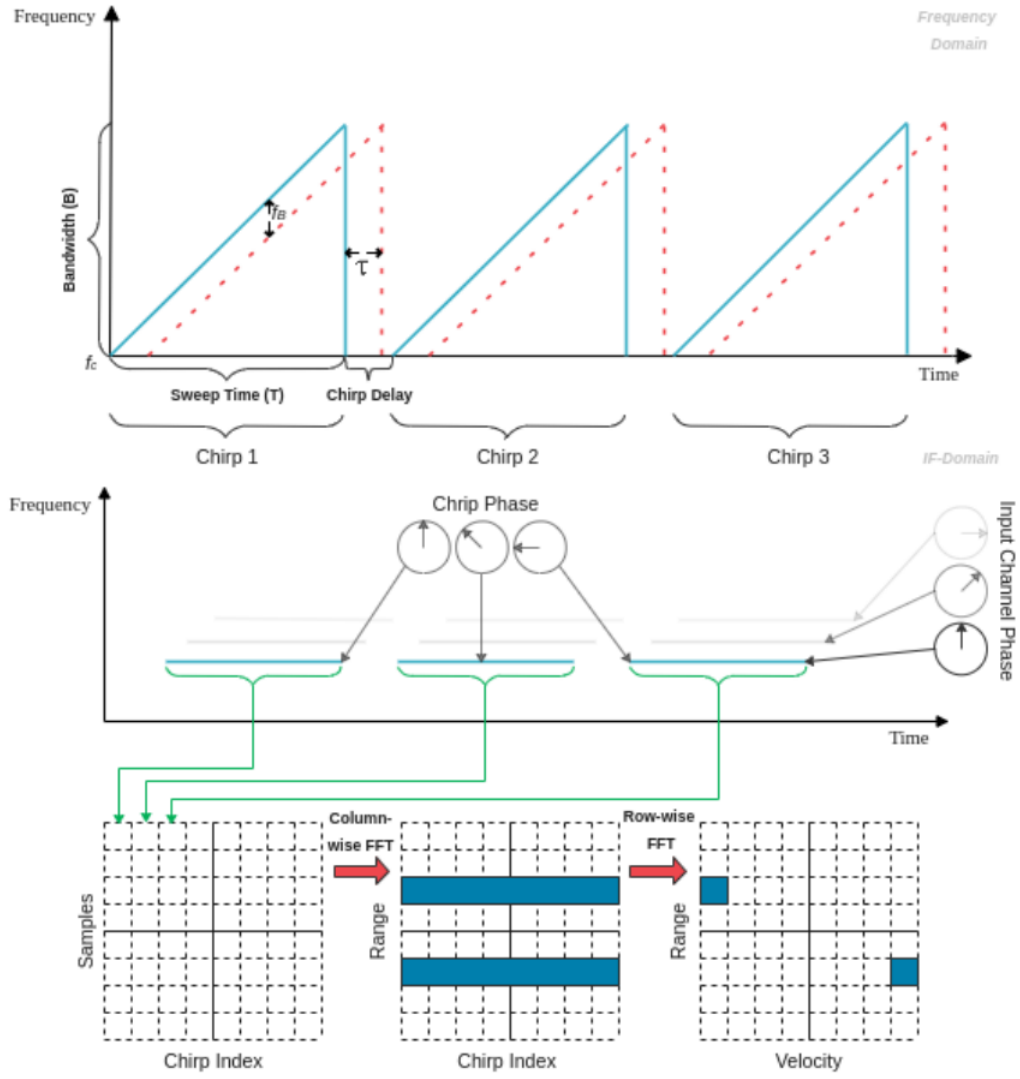

Figure 2.7: Range and Velocity FFT. [21]

Angle of Arrival Estimation

To calculate the angle of arrival (AoA) to a target an array of receiving antennas can be used. The AoA can then be calculated due to the signal having to travel $d \cdot \sin(\theta)$ more distance when comparing antenna 1 and 2. This extra distance causes a phase shift between the two measured signals which can be used to calculate the AoA. [20]

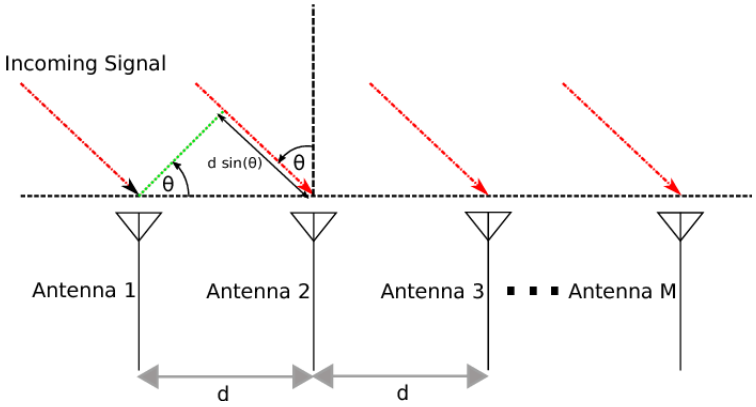

Figure 2.8: Illustration of how the Angle of arrival is defined and calculated. [22]

$$\theta = \sin^{-1}\left(\frac{\omega\lambda}{2\pi d}\right), \tag{2.11}$$

where ω is the phase, θ is the angle of arrival and d is the distance between two receiving antennas.

The angle resolution is the minimum angle separation between two object, for them to appear as two peaks when conduction angle-FFT. The formula for calculating the angle resolution is seen in equation 2.12. [20]

$$\begin{aligned} \Delta\omega &= \left(\sin\left(\theta + \Delta\theta\right) - \sin\left(\theta\right)\right) \\ &\approx \frac{2\pi d}{\lambda}\cos\left(\theta\right)\Delta\theta \\ \Delta\omega &> \frac{2\pi}{N} \\ \Rightarrow \frac{2\pi d}{\lambda}\cos\left(\theta\right)\Delta\theta &> \frac{2\pi}{N} \\ \Rightarrow \Delta\theta = \theta_{res} &> \frac{\lambda}{Nd\cos\left(\theta\right)} \end{aligned} \tag{2.12}$$

The resolution is often calculated with $d = \frac{\lambda}{2}$ and $\theta = 0$, as it is the optimal case for AoA resolution. I results in the following equation: 2.13. [20]

$$\theta_{res} = \frac{2}{N}, \tag{2.13}$$

where θ is the angle to the target, N is the number of receiving antennas and $\Delta\theta$ is the difference in θ based on the distance between the receiving antennas.

The maximum AoA also called the field of view, is restricted by the maximum phase ω which has a maximum value of π radians. Therefore the maximum AoA that can be calculated is defined by Equation 2.14, seen below.[20]

$$\theta_{max} = \arcsin\left(\frac{\lambda}{2d}\right) \tag{2.14}$$

To achieve the largest field of view possible, the distance between the receiving antennas d, should be set to $d = \frac{\lambda}{2}$. See Equation 2.15. [20]

$$\theta_{max} = \arcsin\left(1\right) = \pm\frac{\pi}{2}\text{radians} = \pm 90^{\circ} \tag{2.15}$$

2.1.4 In-phase And Quadrature Components

If only the beat frequency is directly measured with an ADC converter the phase information of the complex signal is lost. By shifting the signal by 90 degrees the imaginary part of the signal can be measured and then analysed. With the In phase and Quadrature signals the amplitude and phase can be calculated by using Equations 2.16 and 2.17. The movement direction of a target can be seen by measuring which signal is leading in phase. [23] [24]

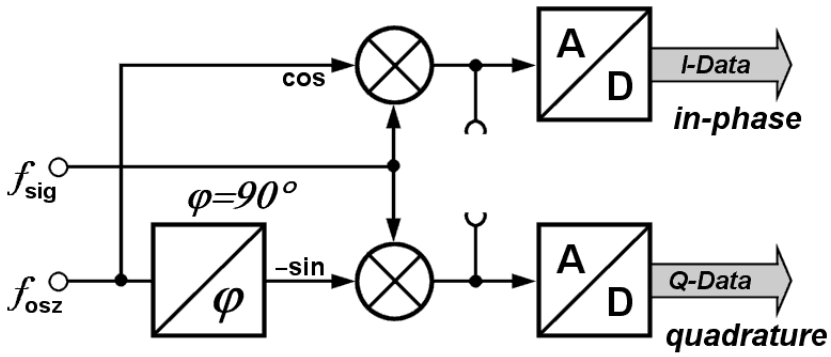

Figure 2.9: In-phase and quadrature principle. [23]

$$A = \sqrt{I^2 + Q^2} \tag{2.16}$$

$$Phase_{IQ} = arctan(Q/I), \tag{2.17}$$

where A is the amplitude of the I and Q signal, I is the signal amplitude of the In-phase component, Q is the Signal amplitude of the quadrature component and $Phase_{IQ}$ is the phase between the I and Q signals

2.1.5 Crosstalk

Due to the close proximity of the receiver (Rx) antenna and transmitter (Tx) antenna on some types of planar radar antennas, the crosstalk signal will be a significant component of the received signal. The range between the Rx and Tx antennas is quite short and this means that the travel time also is short. Because of this the change in the received signal and the transmitted signals frequency will be low. This will cause a low beat frequency with high amplitude. Because of this, there will be a minimum range that the radar can detect objects. [25]

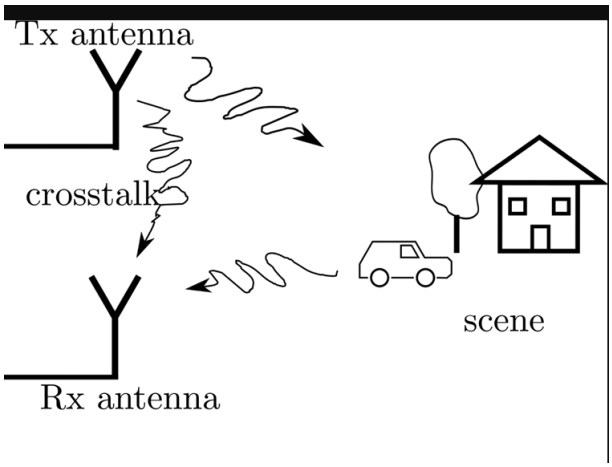

Figure 2.10: The crosstalk is illustrated as the arrow going from the Tx to the Rx antenna. [26]

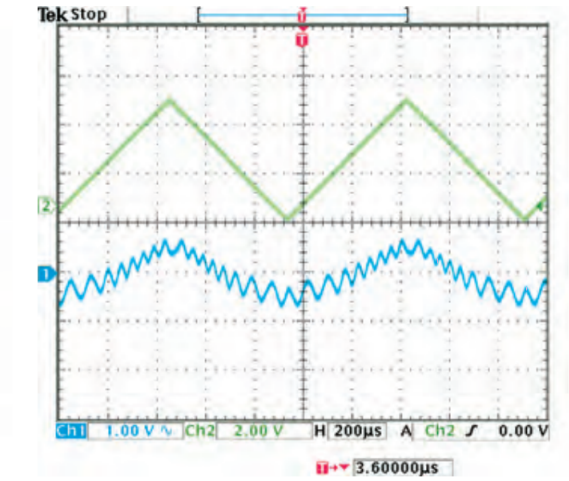

Figure 2.11: Example of how crosstalk affects the signal. The green signal is the unaffected signal and the blue is the affected one. [25]

2.2 Control Theory

In the following section the characteristics of the voltage controlled oscillator (VCO) is presented. After that, the control method phase locked loop (PLL) is described. It is the most common way to control a VCO. Subsequently, an alternative control method, the Proportional-Integrating-Derivative controller will be explained.

2.2.1 VCO

A VCO or "Voltage Controlled Oscillator" is an electronic oscillator that is controlled by a voltage source. The sinusoidal curve created by the VCO can have oscillation frequencies in the microwave spectrum and depending on the tuning voltage the oscillation frequency can be changed rapidly. The VCO can therefore be used in radar applications as the signal source and the variability of the frequency is useful for for FMCW radars that use chirps.

The VCO's voltage to frequency conversion is not a linear function and it is also highly temperature dependant. The cause of these irregularities depends on what type of structure the VCO has, however both of them often exist to some extent. Both the temperature dependency and the non linearity of a generic VCO can be seen in Figure 2.12.

Due to the regulation of the microwave bands that are allowed to be used for radar applications the radar chirp should not pass below or above these frequencies.

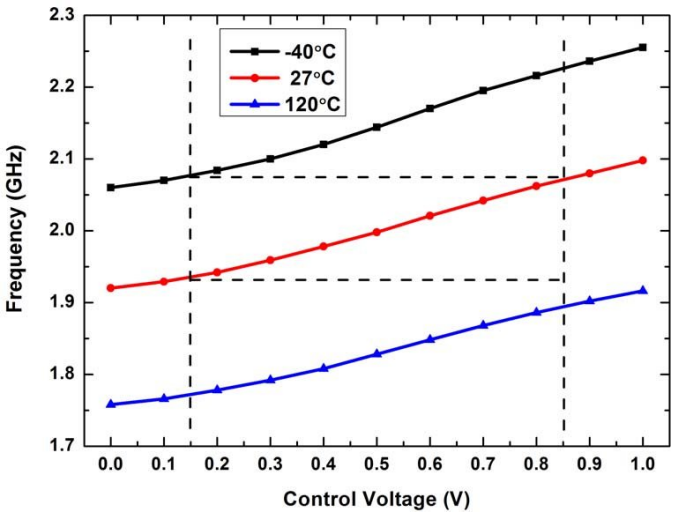

Figure 2.12: Typical VCO Characteristics, including both the non linearity and the temperature dependency. [27]

The non linearity of the VCO affects the beat frequency of the radar chirp and this distorts the measurement accuracy of the radar. As can be seen in Figure 2.13 the non linearity of the VCO will cause the beat frequency to change over the chirp. The usage of the beat frequency and the slope in the calculation of the range to a target is depending on it to be linear. Therefore this non linearity has to be removed to ensure that the beat frequency corresponds to the target that is being detected. Because of

these two factors a control system is required to be able to use the VCO to its highest potential.[28]

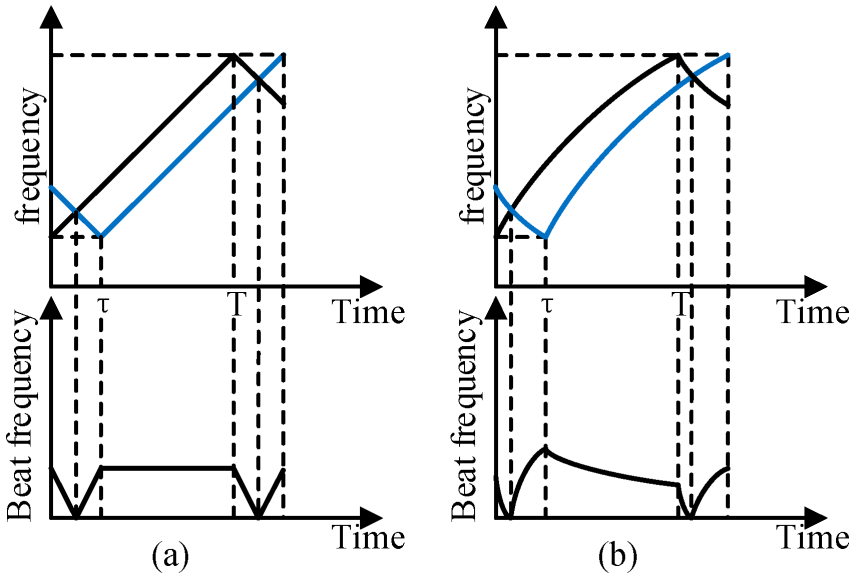

Figure 2.13: Beat frequency of a linear and a non linear chirp. To the right is the linear and to the left is the nonlinear. [29]

2.2.2 Phase Locked Loop

One of the most common ways to control a VCO is with the use of a Phase Locked Loop (PLL). As implied by its name the PLL "locks" the phase of the two inputs F_{IN} and F_F and when the phase is at a stable value the two signals has to have the same frequency. This can be used in conjunction with a frequency divider so that the output frequency is a multiple of the input frequency. The phase lock can be done extremely quickly and if the reference is changed in a continuous way the phase lock will cause the output to also be changed continuously. This makes the PLL a suitable way to generate a radar chirp. By using a PLL to control the VCO the type of input is changed from a DC tuning voltage to a frequency reference input. To generate this input some other type of controllable oscillator has to be used combined with the PLL. An example of the PLL loop is illustrated in Figure 2.14 below. [30]

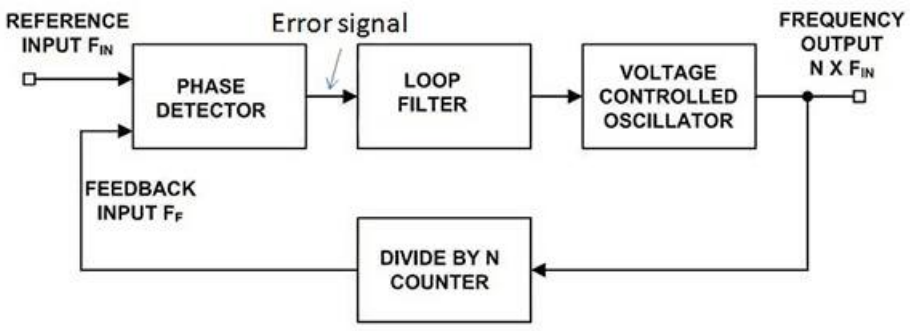

Figure 2.14: Phase Locked Loop. [30]

2.2.3 Proportional-Integral-Derivative (PID) Controller

Another way of controlling a process is the Proportional-Integral-Derivative (PID) controller. It is one of the oldest controller types and the most widely utilised in the industry. It is based around a control error e, which is generated by subtracting a measured output y to a reference value r. When the control error is zero, the measured output signal is the correct value. Generally known for its simplicity and robustness the PID is a versatile controller that can solve many types of problems. The continuous time representation of the PID controller can be seen in Figure 2.15 and Equation 2.18 [31].

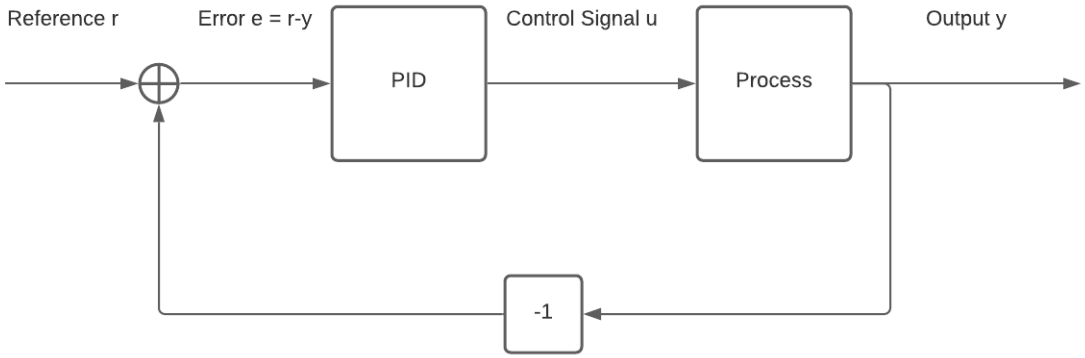

Figure 2.15: Proportional-Integral-Derivative Controller.

$$u(t) = K_p e(t) + K_i \cdot (\frac{1}{T_i} \int_0^t e(\tau)d\tau) + K_d \frac{de(t)}{dt}, \quad e(t) = r(t) - y(t) \tag{2.18}$$

The three parts the PID controller is based on are the proportional, the integrating and the derivative part. All the parts manipulate the control error in different ways. A description of the parts will be given below[31].

Proportional Part

The proportional part acts on the error by amplifying it with a factor K_p. The size of the factor determines its effect on it if its large the controller becomes faster but less stable. If K_p is small the controller becomes slower but more robust to external noise. However, regardless of the factor K_p's size a pure P controller will always result in oscillations and a stationary error[31].

Integrating Part

To counteract oscillations an integrating part is often added to the controller. The integral in the controller sums up the control errors over time and amplifies them with the factor K_i. The result of this is that the stationary error is removed. The parameter T_i limits how fast the stationary error is removed, a small value results in faster removal however worse stability and the opposite for large values [31].

Derivative Part

The last part of the PID controller is the derivative part. The derivative part is used to predict the behaviour of the control error, this is done by derivation of the control error. The derived error is multiplied by the factor K_d, and if tuned correctly it can prevent overshoot. In industrial applications the derivative part is often not necessary[31].

3 Design

The Design chapter is divided into four parts, Design Specifications, System Layout, Design of Control Loop and Implementation On Evaluation Board. The focus of the Design Specification chapter is to introduce the goals with the project and how they were decided on. The System Layout section aims to present the hardware that was designed for the FMCW radar. Different functionalities of the setup are also described in this section. In the Control Loop chapter, it is described how the control method and the sampling method were evaluated and chosen. The section also describes how the sampling and control method was simulated and how the implementation of them were performed on the hardware described in the chapter System Layout.

3.1 Design Specifications

The main component of the project, a 24 GHz radar module from Innosent was provided to us by our supervisors from Axis. The design of the radar module is based on a 24 GHz VCO and a set of planar antennas, contained in a small module that can be directly soldered to a PCB. The Radar module contains a VCO, Rx and Tx antennas, amplifiers, and mixers. The exact components contained are not available, but the general functionality can be derived from the datasheet.

When designing a radar, parameters as range, velocity and angle of attack are important factors that have to be considered. The parameters are limited based on maximum value and maximum resolution for range, velocity and AoA. For a radar with the purpose to replace a PIR movement sensor, the following requirements were decided on as specifications. As the radar module only has one receiving antenna, the AoA is not considered.

- Range Maximum: 10 m (maximum range from datasheet)
- Range Resolution: 0.75 m (maximum bandwidth)
- Velocity Maximum: 4-7 m/s (average velocity of a biker)
- Velocity Resolution: 1-2 m/s (distinguish a biker and a pedestrian)

The following table shows the theoretical limitations for the solution implemented on the evaluation board. The formulas used for the calculations are from section 2.1.3 and the following values are used:

- $c_0 = 3 \cdot 10^8 m/s$
- $f_{BW} = 200MHz$
- $f_s = 4 \cdot 10^5 Hz$
- $\frac{df}{dt} = 1MHz/\mu s$
- $\lambda = 0.0125m$
- $T_f = 0.004s$
- $T_c = 0.0002s$

	Formulas	Value	Unit
Range Resolution	$\mathrm{R}_{res} = \frac{c_0}{2B}$	0.75	[m]
Range Maximum	$\mathrm{R}_{max} = \frac{f_s c}{2S}$	59.95	[m]
Velocity Resolution	$\mathrm{v}_{res} = \frac{\lambda}{2T_f}$	1.55	[m/s]
Velocity Maximum	$\mathrm{v}_{max} = \frac{\lambda}{4T_c}$	15.52	[m/s]

The theoretical range resolution is 0.75 meters and can not be changed since it is dependant on the bandwidth. The theoretical maximum range is 59.95 meters and can be increased by increasing the sampling speed of the ADC. Considering the radar is supposed to substitute a PIR sensor both the range resolution and the maximum range are considered to be good values.

The theoretical velocity resolution of 1.55 m/s could be sped up by increasing the frame size, however since it would cause problems with the RAM memory and a resolution higher than 1.55 m/s is not useful for the application, it was kept at 1.55 m/s. The velocity resolution is reasonable for comparing two bicycles however for comparing two pedestrians walking it is considered low, since it often do not differ 1.55 m/s between the velocity of two walking pedestrians. The maximum velocity 15.52 m/s is considered a reasonable maximum for both walking pedestrians and bikers. In comparison to a PIR sensor the feature to measure velocity is added functionality and therefor considered as an improvement.

3.2 System Layout

The System Layout section introduces the layout of the designed prototype. Afterwards, different functionalities of the MCU is described and also how it is implemented in the prototype. Finally, the self-designed hardware used in the prototype is presented.

To define the system requirements the datasheet was analysed and some key factors were defined. A feedback signal with the frequency of around 3 MHz had to be measured for the control system to work, this meant that some type of frequency measurement had to be devised. The VCO was controlled by an input called Vtune, which had to be controlled accurately at high speeds for the FMCW Chirp. The Vtune input had an accepted input range of 0.7-2.5 V and the conversion rate of the voltage input to frequency output was stated as 700 MHz/V. With a bandwidth of 200 MHz this gave a voltage change of about 0.28 V had to be generated over a short time span and with a high degree of accuracy to ensure a linear chirp [32].

The beat frequency output from the radar had to be sampled with a sampling frequency that gave a high radar resolution and a range of at least 10 m, this is the maximum distance stated in the radar modules data sheet. The voltage level of this signal had a peak to peak level of 250 mV.

With these facts a system layout could be created, 3 hardware parts excluding the radar module were needed for the project. A MCU to handle the control loop and DSP, a low pass filter to increase linearity of the control signal and an active band pass filter to amplify the beat frequency amplitude and reduce noise.

The full system layout can be seen in figure 3.1. The figure contains four parts, the MCU to the left, an RC-filter and an active bandpass filter in the middle and the radar module to the right. The upper section in the figure is the control loop and the bottom section is for the DSP.

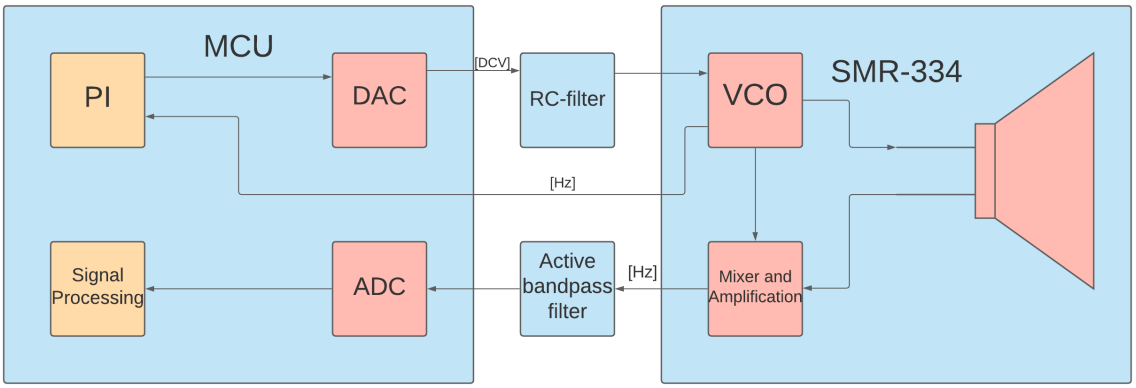

Figure 3.1: System Layout of the prototype.

3.2.1 MCU

Careful evaluation of which type of MCU had to be done to ensure that the MCU could handle both the control loop and the data used in the radar DSP. A number of main factors and functions were investigated and minimum requirements were set.

Clock speed

One of the most important factors for the MCU were the clock speed of the MCU. There had to be enough to be able to do the required calculations for the DSP while simultaneously be able to control the radar module. But since this is heavily dependant on how the code is implemented it is hard to calculate a minimum requirement. The clock speed also has a big impact on a frequency measurement of the feedback signal if it is done with a timer. There are two factors related to the frequency measurement - oscillation frequency and accuracy of the clock speed. The maximum clock speed frequency depends on the MCU, but the accuracy depends on the source of the oscillation frequency. To ensure a high degree of accuracy an external high speed crystal was used. This gives a high accuracy for a low cost as they are a common component.

Price

One of the main reasons to use a digital control method for the VCO is to reduce the price of the total system price by eliminating the total amount of components, therefore the use of a cheaper MCU is an important factor to consider.

ADC

To be able to read the analogue data sent from the radar some type of analogue to digital conversion has to be done, the speed and resolution of this affects the accuracy of the data collected from the radar. The sampling frequency has to twice as high as the maximum beat frequency that the radar will have to detect due to the Nyqvist frequency criterion.

DAC

A way of controlling an analogue part with a MCU can be done with a digital to analogue converter, the speed and resolution of this affects the accuracy of the control signal for the radar. the speed that the DAC can change its output value is extremely important for the project due to the importance of a quick chirp which is directly correlated to the velocity measurement. It also has to be able to change the control signal in small enough steps to counteract the non linearity.

Memory

The DSP required for the radar data can use relatively high amounts of memory for a low end MCU, due to this some thought has to be taken to not run out off RAM when doing the DSP.

3.2.2 Evaluation Board For MCU

To be able to test the entire system without creating a PCB an evaluation board can be used. The evaluation is a development platform that is used to test a certain part and in this case a MCU. This comes with the advantages of being easy to use and it can also have a dedicated MCU for debugging purposes. Due to the need for an accurate external clock for the accuracy of the frequency calculations, the evaluation board was modified to have a high speed oscillator. The largest downside with using an evaluation board is that it requires cables and non-ideal connectors for the filters and radar module. This can increase the effects of EMI which can affect the signal integrity.

3.2.3 Active Band Pass filter

An Active band pass filter to reduce high frequency noise from IF-signals, but also to amplify the signal to get better accuracy from the ADC. The active band pass filter does several different things to make the signal as suitable for the ADC as possible. Since the unfiltered signal is centred at around the 1-2 V range with a peak to peak range of 100-200 mV. Since maximum voltage for the system is 3.3 V it would limit the gain to less than 2 to ensure that the supply voltage is not exceeded. To circumvent this problem the high pass part of the band pass filter was used, not to reduce low frequency noise but instead to remove the DC component of the signal. Thereby reducing the signal to a 100-200 mV peak to peak centred around 0 V. This signal could then be amplified by a larger amount and still not pass above the supply voltage. Since the DC-block puts the signal at a working point of 0 V the signal will sometimes be at below 0 V and this cannot be supplied without a negative supply voltage. To counteract this the working voltage of the amplifier can be set to the midpoint between 0 and 3.3 V. This causes the signal to be centred around 1.5 V with a signal peak to peak of 1-2 V that can be read by the ADC.

There are several important factors when deciding on the operational amplifier for the active filter. However, the most important will be the *slew rate* for this application, this is the maximum rate change of the output of the operational amplifier. To not distort the signal it is important to have a slew rate that is higher than the required maximum change of voltage. This will depend on both the beat frequency and the magnitude of the signal.

To test the filter design before building it was simulated in LT-Spice and the schematic of this can be seen in Figure 3.2.

3.2.4 Low Pass Filter

The DAC of the MCU will output the voltage level in discrete voltage levels, this causes the control signal to the VCO to look like a staircase function, as can be seen in Figure 3.3. This decreases the linearity of the function and will lower the accuracy of the radar. To counteract this a low pass filter can be used to smooth out the steps of the control signal and make the discrete signal a continuous signal. This filter can

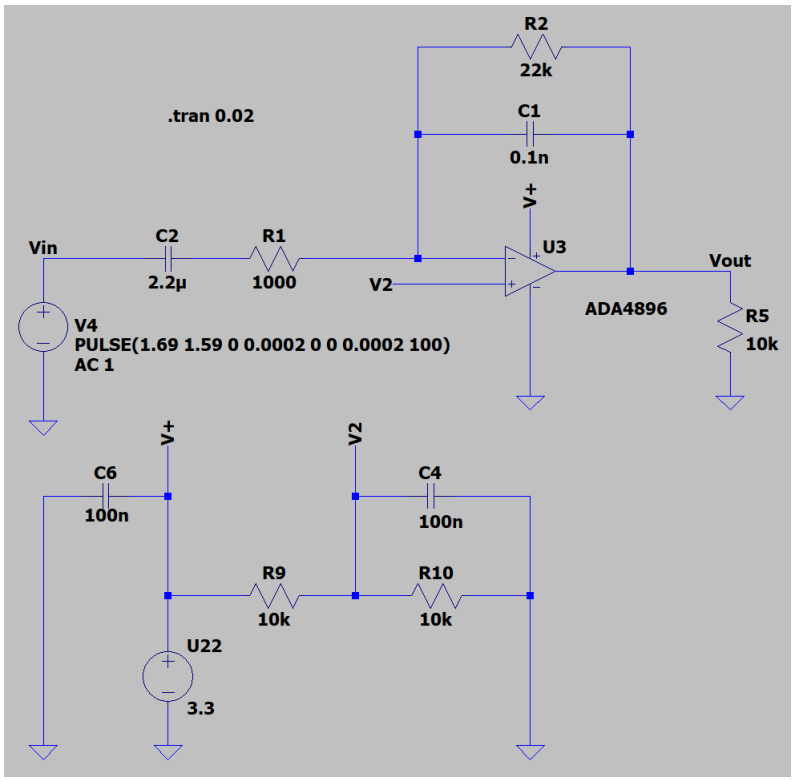

Figure 3.2: Active Bandpass Filter Schematic.

be simulated in simulation software like LT-Spice for the initial component tests and then further refined by testing. The main parameters to take into consideration when simulating the filter are the number of steps, time until the next step and the voltage change per step.

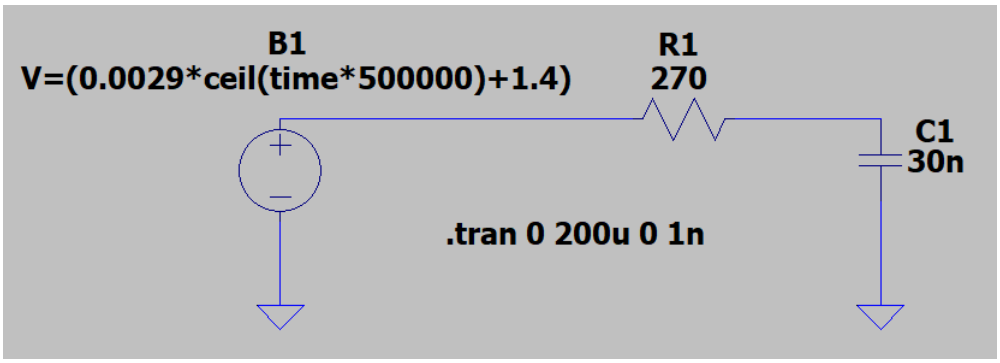

Figure 3.3: Low pass filter Schematic.

3.3 Design of Control Loop

The main objective with the control loop in this thesis was to control the non-linear and temperature-dependent VCO. In the following subsections, the workflow to meet these requirements will be described. Starting with different methods for sampling frequency. After that, by a Simulink model for investigation design choices and after that how the solution was implemented on the evaluation board.

3.3.1 Frequency Measurement

To be able to design a functioning solution a proper way of sampling the VCO's output frequency had to be decided on. Two ways of measuring frequency were therefore investigated, direct frequency counting and reciprocal frequency counting.

The two methods are supposed to measure a frequency of roughly 3 MHz. The reason for the frequency being 3 MHz and not 24 GHz as the radar is operating in, is because the signal from the radar is down converted by 8192. This is done in the radar module and the reason for it is because it is easier to measure a lower frequency of 3 MHz instead of 24 GHz.

Direct frequency counter
: It is a common way to calculate the frequency. This works by letting the MCU increment a counter each time a rising edge is detected and then when a specified and known amount of time has passed the frequency can be calculated as the number of edges divided by the counting time.

Reciprocal frequency counter
: Is a method where the time between two edges is used to calculate the frequency. This has the advantage of having a resolution that is dependant on the master clock frequency. Whereas the Direct frequency counter is dependant on the counting time.

As the methods were investigated, it was decided to implement the reciprocal frequency counting on the evaluation board. This, seemed the most appropriate method for sampling the high frequency that was desired.

3.3.2 Simulink Model

When the method for sampling frequency was decided, a Simulink model was designed. The reason for making this model was to evaluate the method for sampling the VCO's output frequency and to evaluate different control methods for controlling the VCO. However, the intention with it was also to be able to determine requirements that had to be satisfied by the hardware.

Full Model

The Simulink model that was designed can be seen in Figure 3.4. The top part of the figure represents the digital sampling of the VCO's output frequency and the bottom part represents the control method. The model was designed in two steps, first, the control loop was designed from the reference signal to the VCO's output, connected with a simple feedback. After that, the method for sampling was constructed and the two parts were put together by substituting the feedback by the sampling part. Now a description of the two parts will follow, starting with the control part.

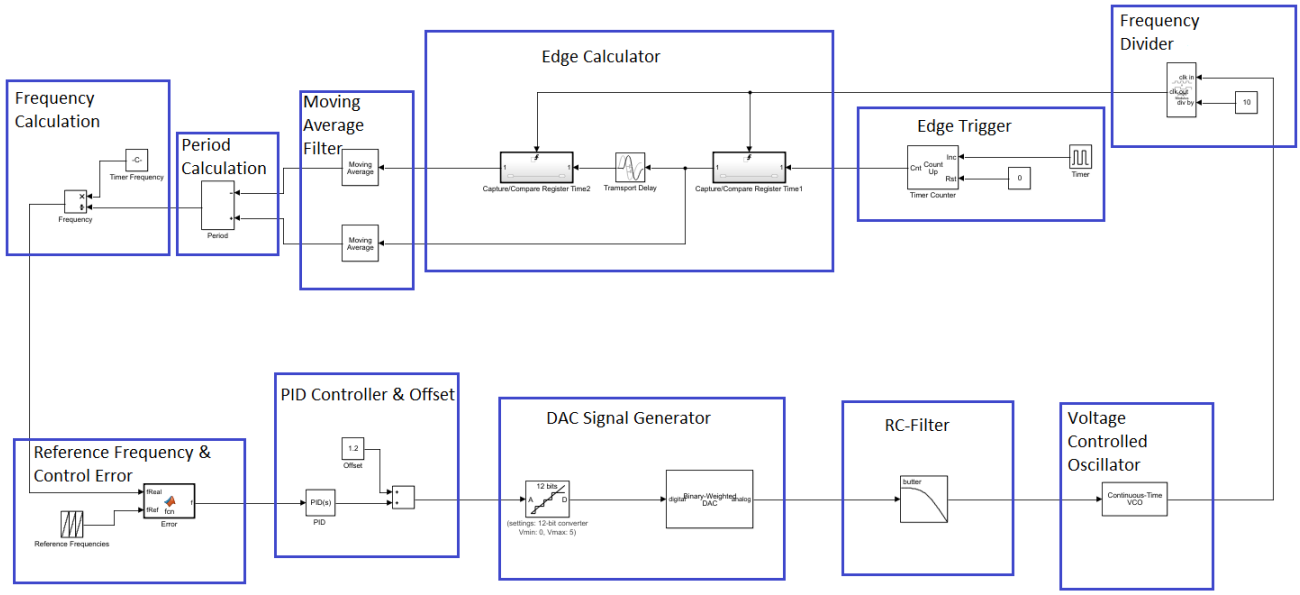

Figure 3.4: Simulink setup for the control loop.

Reference Generation & Control Error

Starting in the bottom left corner of the model, the reference frequencies were generated from a sawtooth waveform and were generated in continuous time. The reason for the frequencies being in continuous time was because the control block that was used, ran in continuous time. To the right of the reference waveform, there is a Matlab function block and it is used to calculate the control error. It has two inputs, the reference frequencies and the measured frequencies. By subtracting the measured frequencies to the references, the control error is established. The real frequencies are a sampled representation of the output signal from the VCO and will later be described in more detail.

PID Controller & Offset

After the control error was calculated it was used as the input signal to the PID control block. Initially, it was decided to use the PID control block as a control method, because it is the simplest form of controller. The PID controller was tuned by setting the size of three parameters, the proportional, the integrating and the derivative amplifications. These parameters were set by trial and error and resulted in only the proportional and the integrating part being needed. Therefore it was decided to use a PI controller, instead of a PID controller. When the PI control signals were calculated an offset was added to them, to counteract an offset caused by the RC-filter.

DAC Signal Generator

After the control signal is calculated, the signal is discretized to resemble how it would appear in an MCU. This digital signal acts as an input to a DAC block. The DAC block is used to output an analogue signal from an MCU and this block is, therefore, a representation of that. Since the DAC was used to make the signal analogue, it will appear as a staircase function in voltage.

RC-Filter

To counteract the staircase behaviour of the DAC block an RC-filter was used. The filter smooths out the steps, resulting in them appearing as continuous.

Voltage Controlled Oscillator

The output of the RC-Filter acts as the input signal to the VCO block. As the voltage is processed by the VCO, it is transformed from a voltage change into a frequency change, which will act as a chirp. The VCO block that was used in the Simulink model did not have the exact same characteristics as the one used in the radar module. However, out of the two VCO's available in Simulink, the one chosen was most similar to the real VCO and therefore it was decided to use it in the model.

Frequency Divider

The sampling part of Figure 3.4, starts in the top right corner. A frequency divider is used to lower the frequency of the VCO's output by a factor. This method can be used when working with high frequencies because it is easier to sample lower frequencies, however it comes with the downside of decreased accuracy. In the model, it was also used to speed up the execution time in Simulink, due to smaller numbers in the calculations.

Edge Calculator & Edge Trigger

To the left of the frequency divider, there are two blue boxes, called *Edge Calculator* and *Edge Trigger*. These parts in combination are a representation of how it was intended to sample a frequency with an MCU. Starting in the left box, there are two capture compare blocks, which both have the down-converted signal as their inputs. The capture compare blocks also have a trigger and an output.

How the output signal behaves depends on how the capture compare block is triggered. The trigger signal is generated from a timer block and a count up block. The timer generates a square wave at a predetermined frequency and the count up block generates a spike at each positive edge.

The spikes are used as a trigger signal to the right capture compare block, resulting in one sample of the dividers output signal. After that the output of this block is delayed by a unit delay and used as the trigger for the left capture compare block, resulting in another sample of the signal. When the first two values are sampled, the process continuous for the whole chirp, resulting in a discrete representation of it.

Moving Average Filter

To calculate the frequencies accurately a moving average filter was used for both of the capture-compare blocks outputs. A fixed value of samples were averaged, this method was used to make the values reliable.

Period Calculation

After the values were averaged, the first edge is subtracted by the delayed one. By doing this the period of the signal was achieved. This is also done for the whole chirp signal, like the rest of the process.

Frequency Calculation

When the period was calculated the frequency of the chirp is calculated. This, by taking the value divided by the period, that was previously calculated. As for the sampled values this is repeated for the consecutive chirp. All these frequencies are what previously were referred to as the real frequencies, which were used to calculate the control error.

Evaluation of Model

As was mentioned at the beginning of the chapter, the idea was to use the simulation to evaluate different methods for evaluating different control methods for linearizing

the VCO and to determine requirements that has to be satisfied by the hardware. However, due to multiple changes between discrete time and continuous time, the model became slow and therefore could not be used for all of this. It gave a reasonable estimation of the clock speed requirement of the MCU and it could be used to validate the sampling method described above. It could also be used to determine that only the proportional and integrating part of the PID controller was needed. Evaluating other control methods proved difficult due to the long simulation time for the model and the PI controlled was deemed sufficient for the project.

3.4 Implementation On Evaluation Board

After the Simulink model was evaluated, the sampling and the PI controller was implemented on the evaluation board. The following sections will give a brief explanation of how the controller was implemented and afterwards a more detailed description of a few improvements that were made to increase the performance.

3.4.1 Full Control Loop

A simplified version of the proportional-integral control structure can be seen in Figure 3.5. The structure can be divided into different parts, as can be seen by the boxes in the model in Figure 3.5. A description of these sections will be given below, starting with the implementation of the control method.

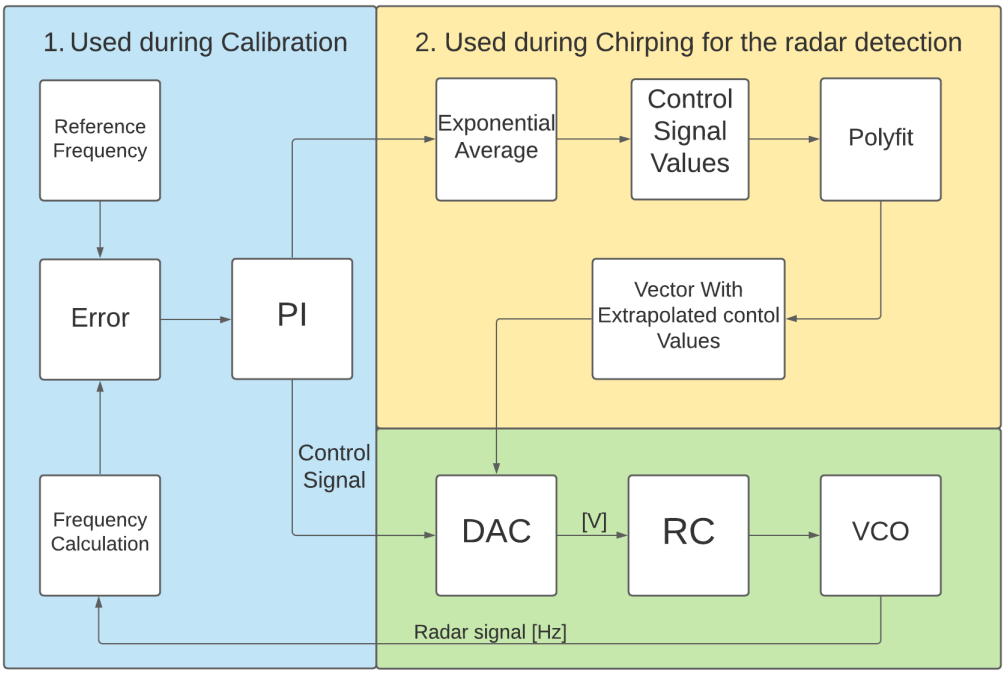

Figure 3.5: Block diagram of the code implemented on the MCU.

Frequency Sampling & Calculation

The sampling of the VCO's output signal was done using reciprocal counting, as was described in Section 3.3.1. The method, as was described earlier is often used to sample high frequency signals and the implementation of it on the MCU resulted in accurate frequency measurements. As the VCO's output signal is a chirp, multiple control signals had to be calculated to create the chirp. The number of reference frequencies was decided based on the number of control signals needed to generate a full chirp.

The reciprocal counting was implemented in the following way. First, a timer with the help of a callback function is used to count 1000 rising edges. As the 1000th rising edge is counted, the timestamp is saved. The timestamp is subtracted by the previously saved timestamp, which the first time is zero. By subtracting the timestamps the period of the signal is calculated. Subsequently, the frequency is calculated by dividing the amount of samples by the clock frequency, divided by the period, see Equation 3.1. The clock frequency value is compensated by the prescaler of the input capture. As one frequency is calculated the timestamp is saved as "previously saved timestamp" and the process is repeated for the whole chirp.

$$Frequency = \frac{\frac{Samples}{ClockFrequency}}{Timestamp2 - Timestamp1} \tag{3.1}$$

Frequency Divider

As mentioned in the system layout section the output signal from the VCO is divided by 8192. The result of this is that the frequencies that have to be sampled are around 3 MHz and not 24 GHz, as is the operation frequency for the radar module.

Reference Frequency

To be able to calculate the control error and subsequently the control signals, the same amount of control references as sampled frequencies had to be generated. Therefore a number of frequency references had to be generated. The reference frequencies were made to create even steps between 24.05 GHz and 24.25 GHz, as this was the ISM Band used for the radar. Since the signal measured is divided by 8192 the reference frequencies were also divided by this amount.

Control Error

The control errors were calculated by subtracting the sampled frequencies to the reference frequencies.

PI Controller

The PI controller was designed by first calculating the control values using the control error. When the control values were calculated they were added together to generate a control signal. To speed up the control loop, an offset was added to the control signal. This, since it makes the control signal start off faster. After that, the control signal was saturation checked to ensure that the control signal did not exceed the maximum allowed voltage of the radar module and afterward saved in a vector that is later used to generate the chirp. This process then is repeated for all control errors.

The derivative part was not used in the implemented controller. The main reason for this was that the derivative part slows down the increase of the control signal, as it is close to the set-point. The result of this is no overshoot if properly tuned, however with the downside of the controller being slower. It was observed that the control action was faster with some oscillations on each set-point. The same was observed with the simulated model as mentioned before.

It was decided to implement a PI controller in the control loop. The reason for not implementing a more advanced controller as the linear quadratic regulator (LQR), was mainly based on the results from the simulated model. It suggested that a PI controller would be a sufficient control method and as the implemented Simulink model was too slow to implement any other control method, it was not investigated further. It was however discussed if it would be beneficial to implement an LQR, but decided that it would be to complex to do it for this solution. It would require a lot more modelling and was therefore concluded too time consuming, as it could not be confirmed to be a better solution than the PI controller beforehand.

Calibration

The process of continuously sample multiple frequencies and calculating control signals was deemed to be too slow. Therefore it was decided not to calibrate the control signals continuously but instead calibrate at decided times. By doing a calibration of the control values before starting the chirping both the non linearity and the temperature dependency could be counteracted. It comes with the problem of a downtime caused by the need to turn of the radar during the calibrating, compared to PLL which is a system that continuously calibrates with the phase lock and therefore avoids this problem. Therefore the calibration needs to be quick to minimise this downtime. There have to be systems in place to determine when to calibrate as well. The two main causes to calibrate were determined to be due to general frequency drift caused by the instability of the system and changes in temperature. This meant that the calibrations should be done after a set amount of time or a temperature change. The time required for the calibration has several dependencies - how the code is implemented and how many control values have to be calibrated.

DAC Output & RC-Filter

The control signals are sent from the MCU on the DAC's output. As its output is digital it generates a staircase function, rather than a linear function. To be able to smooth out the steps a low pass RC-filter was used. This concept worked in the same manner as in the Simulink model.

DMA

To achieve a speed measurement of the radar target with a high resolution it was important to generate a chirp rapidly. This was done using Direct Memory Access (DMA), which is a peripheral that is available for some types of MCU's. This is a way to transfer data over the data bus without the use of a CPU command, this lowers the number of instructions the CPU has to execute. It is done by setting a point in the memory for the DMA to use and connecting it to another peripheral. Two of the peripherals that can be used with DMA are DAC and ADC. Then the CPU only has to trigger the start of the peripheral with some type of trigger.

Exponential Average

To be able to generate stable control signals it was required to make reliable control errors. Therefore averaging methods were implemented for calculating the control error. Two types of averaging methods were evaluated, exponential average and moving average, both of these methods only take into account the most recent values. Moving average saves the values in a first in last out (FILO) vector and calculates the average of the currently saved values in the vector. Exponential averaging adds a percentage of the current error to a percentage of the current average error. Since the average error has to be continuously calculated during the calibration of the radar, the averaging methods calculation time will affect the calibration time in a significant way. The moving average has the large downside of using division which is computationally slow for an MCU. After both of them were evaluated the exponential average filter was chosen, as it performed better.

Polyfit

The calibration time of the radar is heavily dependant on how many control points that the PI controller has to compute. However, a lower amount of reference points will decrease the linear behaviour of the controller due to the larger voltage steps between each control signal. To still have the same amount of control signals but a lower amount of reference points, a quadratic polyfit function was used. The polyfit function is used to extrapolate the calculated control signals to have smaller voltage steps. This decreases the calibration speed while still maintaining a high degree of linearity. As the polyfit function was implemented to the code the sampled real frequencies and the reference frequencies could be reduced by five times. The control signals could still be extrapolated to the same amount of steps as before and therefore the same resolution was achieved, but the computing time could be decreased.

The polyfit function that was used was based on the work from [33] but it had to be modified to work in the system.

4 Results and Analysis

In this section of the report, the results from the different tests are presented and they are all discussed. In Chapter 4.1 the final setup is presented and in Chapter 4.2 results and a discussion regarding the simulations is given. After that, the results from the implementation of the control loop are presented and discussed in Chapter 4.3. Finally, in Chapters 4.4 and 4.5 the results from the tests with the I and Q signals are given and improvements are suggested.

4.1 Final setup

For the created prototype a STM32F410RB Evaluation board was used[34]. This model of the F4 Line of MCUs had good specifications for a relatively low price and was deemed a good choice for the project. With a 100MHz internal clock speed, it could provide a good sample rate for the feedback signal and have a high calculation speed. It also had an Internal ADC and DAC which was required. The Evaluation board was fitted with a protoboard with the Radar module, RC filter, and the Active band-pass filter. The final prototype is seen in figure 4.1

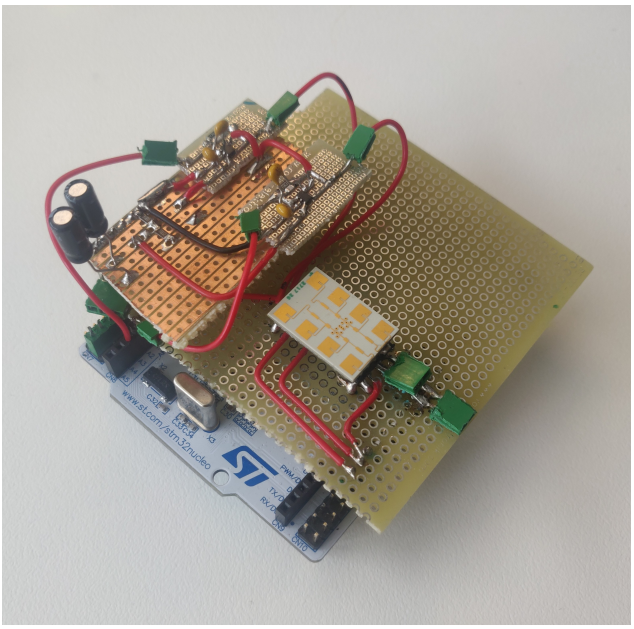

Figure 4.1: The full implementation of the system layout, including the evaluation board, the active bandpass filter, the radar module and the RC-filter.

4.2 Simulation Results

In the following chapter, the results from the Simulink model will be described. Afterwards the results will be discussed and conclusions made from them will be presented. Below is a list of parameters for the model.

- Chirp range: 24.05-24.25 GHz
- The Simulation time for the model is 100 microseconds
- Moving average filter: Number of values 3
- PI parameters: $K_p = 5 \cdot 10^{-6}$ & $K_i = 10^{-2}$

4.2.1 PI Controller

In figure 4.2 the error signal from the Simulink model is displayed. As the measured signal is zero when the simulation is started, the control error becomes large in the beginning of the of it. After $10 \cdot 10^{-6}$ seconds the measured signal is stabilised and the error therefore to stabilise around zero.

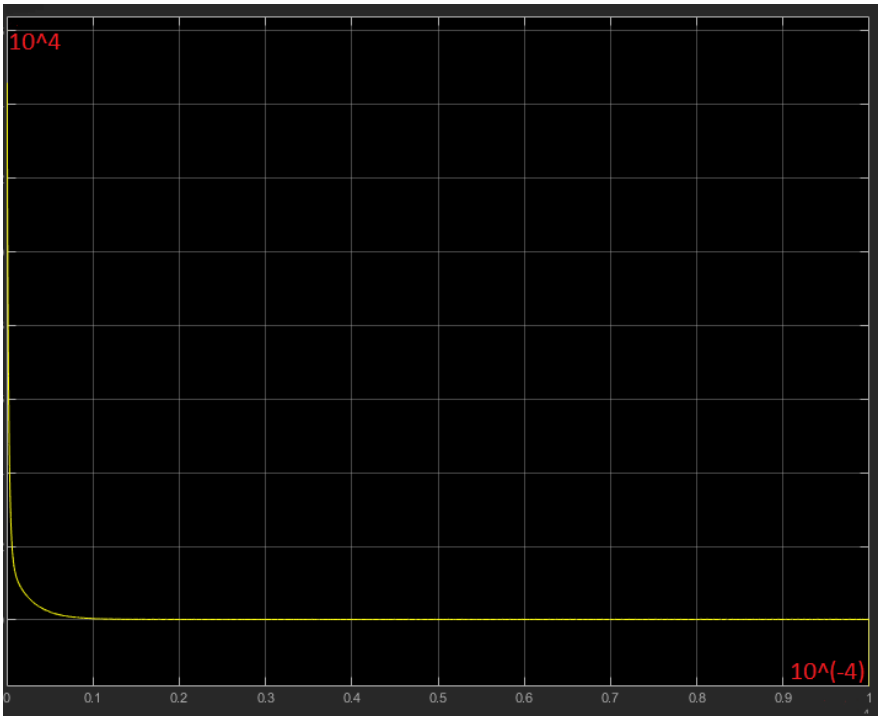

Figure 4.2: The control error from the Simulink model. On the x-axis is time in seconds and on the y-axis is amplitude.

The output signal from the DAC-block and the output signal from the RC-filter are shown in Figure 4.3. The blue line in the figure is the DAC-blocks output signal and the yellow is the RC-filters output. The DAC's output signal is the analogue representation of the control signal. As displayed in the figure the blue signal has an amplitude peak at the beginning of the simulation and that is a result of the RC-filter. The same effect is shown on the yellow line as the slow increase.

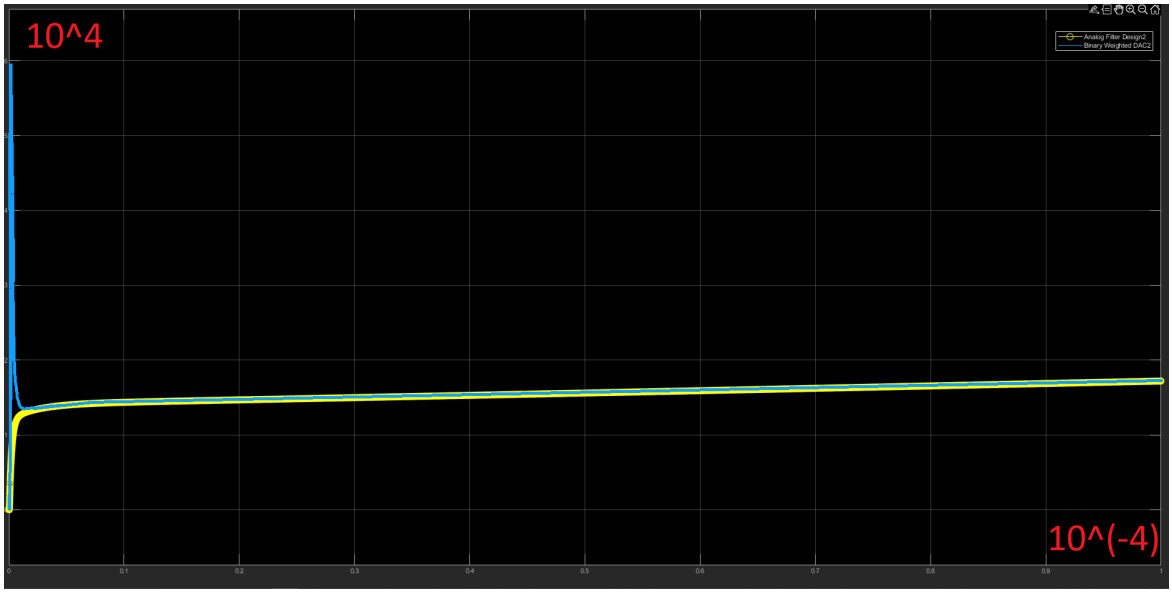

Figure 4.3: The DAC signal before and after the RC-Filter. The blue line is before the RC-Filter and the yellow line is after. On the x-axis is time in seconds and on the y-axis is amplitude.

The chirp, the output of the VCO is shown in Figure 4.4. The chirp ranges from 2.935 MHz to 2.960 MHz which corresponds to 24.05 GHz to 24.25 GHz. The figure is zoomed in for visibility.

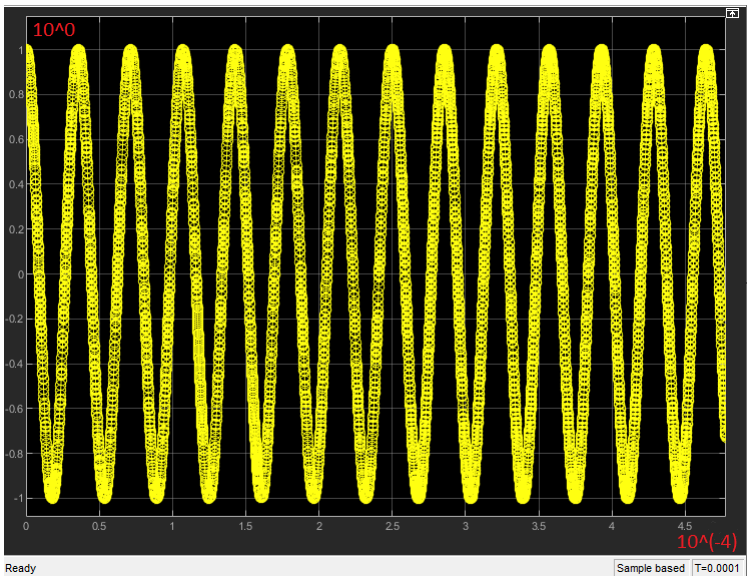

Figure 4.4: Zoomed in chirp from the Simulink model, to illustrate how the chirp looks. On the x-axis is time in seconds and on the y-axis is amplitude.

The generation of the chirp is accurate and ranges between the correct frequencies. It takes approximately 10 microseconds to reach the set-point but that is expected since no controller is instantaneous. The simulation however could not be run for 200 microseconds due to lag in the model. The lag also resulted in the PI controller being the only control method investigated. However, it could be concluded that the proportional and integrating part were the only two necessary to control the VCO. Unfortunately, the parameter values of K_p & K_i could not be used in the real model.

4.2.2 Frequency Sampling

The reference frequency and the sampled frequency can be seen in figure 4.5. The yellow line is the frequency reference and the blue is the sampled signal. The sampled signal uses a moving average filter and the best results were given from using 3 samples.

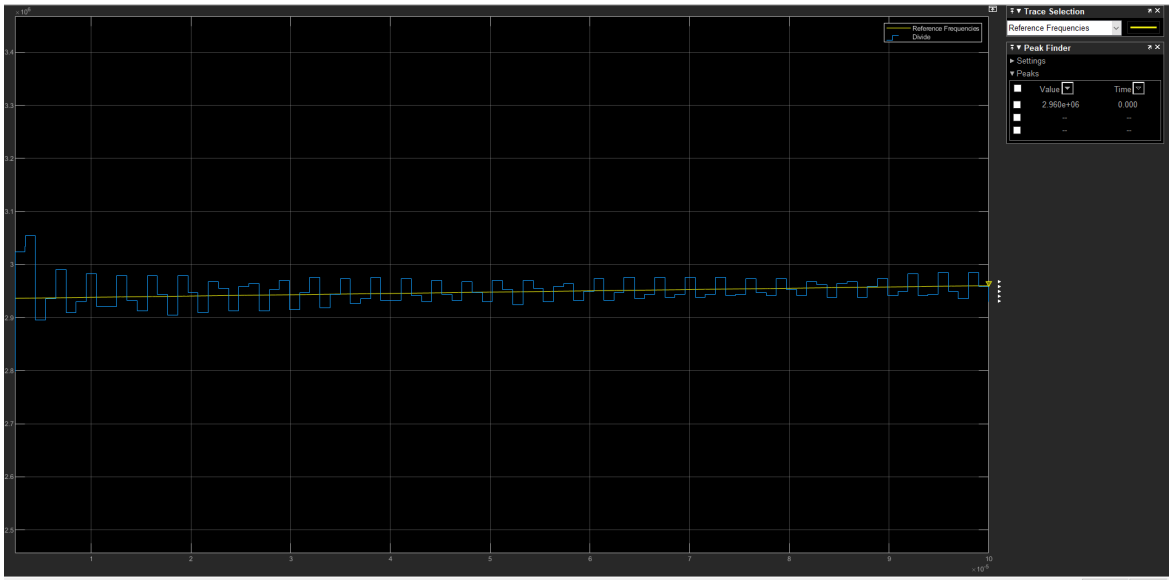

Figure 4.5: The reference frequency can be seen as the yellow line and the sampled frequency as the blue. On the x-axis is time in seconds and on the y-axis is amplitude.

The sampling was largely affected by the moving average filter, used in the model. When the moving average was set to 3 values the frequencies were calculated accurately. The number could however not be used in the real model. Also, this part of the model was highly affected by the lag and the model therefore had to be run slower than intended. Resulting in different parameters not being as useful as they could have been.

Overall, the Simulink model was not as useful as expected for analysing sampling and determining control method. This, mostly due to lag in the simulation which resulted in it taking more time to develop the model. It was possible to determine that a PI controller would be a suitable control method and it gave a indication regarding the sampling method. If this stage of the thesis would be made again, it probably would be better to do it in Python, since Python has a lot of different libraries and is commonly used for different types of simulations.

4.2.3 Filter Simulations

Both of the simulated filter plots for the active band-pass filter and the RC filter can be seen in Figures 4.6 and 4.7. The values for the input signal for each filter had to be estimated based on datasheets and test data. This gave a good starting point for the filters.

As can be seen in the Figure 4.7 the RC filter will cause a small offset to the control signal, this offset can be reduced by adding some value to the control vector. However, to know how much this value show it has to be set manually at the moment. It can also be overcome by simply not sending the last values in the chirp, this would however decrease the bandwidth. No theoretical way of determining the RC filter parameters was found, except to simulate and to test until a good set of components were found.

The inversion of the signal caused by the active band-pass filter can be seen in Figure 4.6. No other filter design could be found that had the same functions with no inversion and the signal can be inverted digitally if required.

Both of the filters worked as intended, some additional fine-tuning for the RC-filter had to be done to get a smoother slope. With correct filter theory and additional testing the linearity could be increased more.

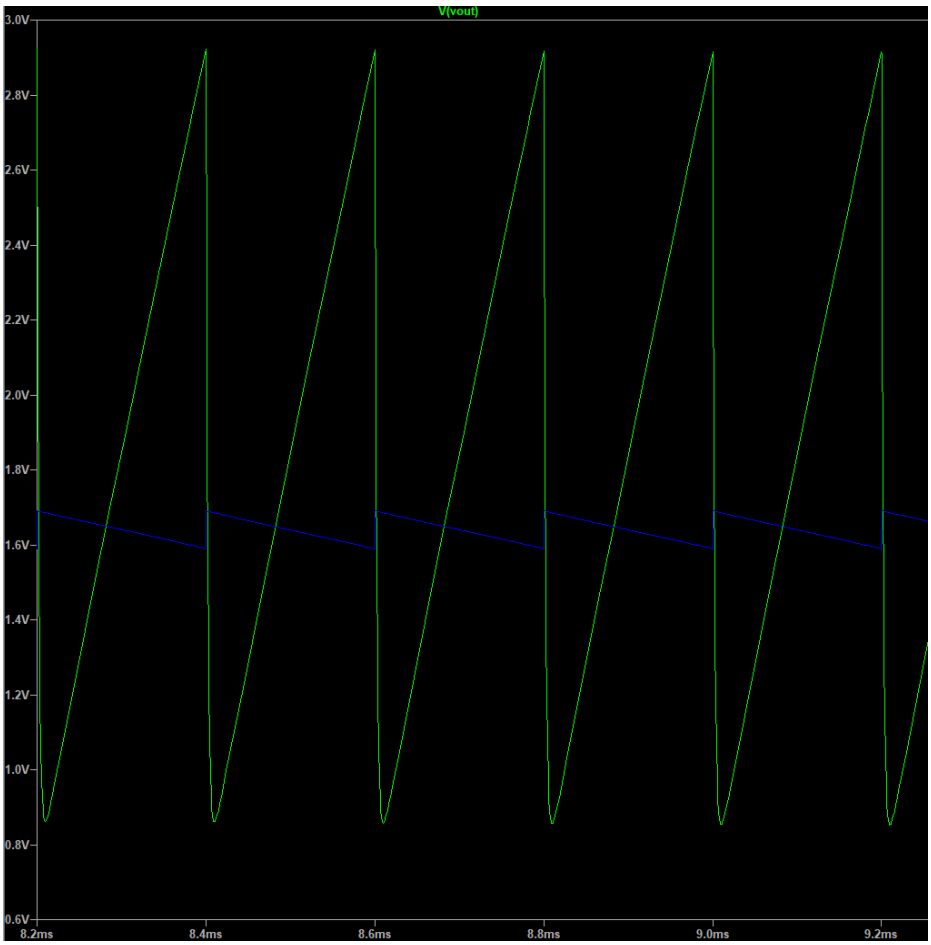

Figure 4.6: Active bandpass simulation. The blue signal is the original and the green is the amplified and filtered signal.

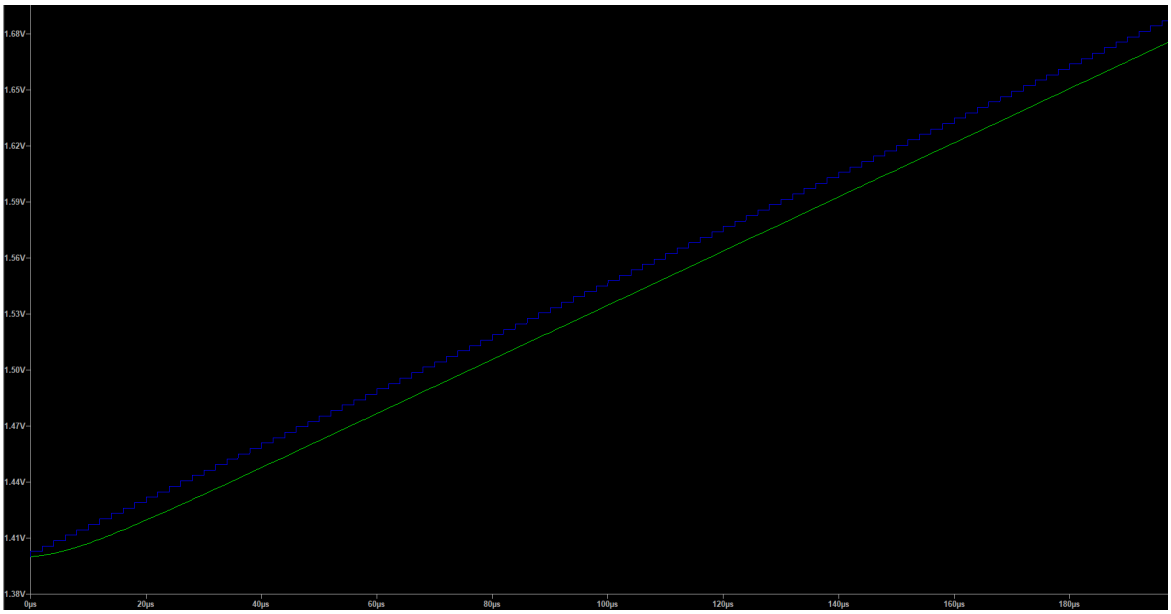

Figure 4.7: RC-filter Simulation. The blue staircase function is without the RC-filter and the green with the RC-filter.

4.3 Evaluation of Control Loop

In this section, the tests done on the implemented system are presented. These tests were done to be able to evaluate the viability of the created system and to ensure that it worked as intended. Before the tests are presented a brief discussion regarding the control parameters is given.

4.3.1 Control Parameters

The PI controller was implemented with the following parameters:

- $K_p = 0.001$
- $K_i = 0.011$
- $Offset = 1928$

As the controller has a low proportional gain, it results in slow control action. However due to the high integrating factor, this was compensated for. The result of the integrating factor is a control signal that increases fast as the control error is large and a control signal that is small when the control error is close to the set-point. The result of this is less overshoot and oscillations. Since the controller has multiple set-points this is the behaviour desired to achieve.

To speed up the controller further an offset was added to the control signal. The consequence of this is that the first control signal does not start from zero but instead has a start value which will start the output at a closer value to the reference value and therefore operate faster.

4.3.2 Frequency Measurement

An important part for the controller is the accuracy of the feedback signal. Two tests were done to verify that the frequency measurement worked as intended with the controller.

First, the DAC was set to a constant value while continuously measuring the frequency with both the MCU and the oscilloscope. The MCU measured the frequency to about 2.935628 MHz ± 10 Hz and the oscilloscope measured an average of 2.935620 MHz with a standard deviation of 50 Hz which can be seen in Figure 4.8.

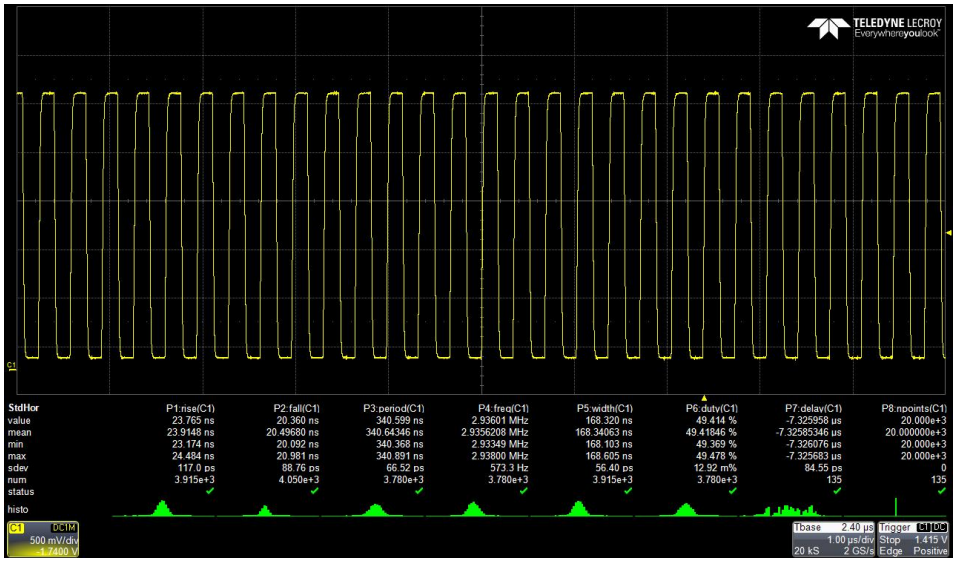

Figure 4.8: Frequency measurement - Static control value.

To test the stability of the PI controller and to see how closely it can match the reference value and the real frequency a test was set up with a constant reference value and then letting the PI control the DAC. With a reference value of 2.935791 MHz the MCU measured 2.935769 MHz ± 30 Hz and the oscilloscope measured 2.935754 MHz standard deviation of 568 Hz, which can be seen in figure 4.9 The control signal is almost directly dominated by the I part of the controller and the P part goes close to 0, the I part will then sit at a quite stable level often shifting one bit.

The conclusion that can be drawn from these tests is that the frequency measurement of the MCU is down to a level of accuracy where the accuracy of the external clock will start to affect the measurements. The PI controller is limited to the accuracy of the DAC and as it is a 12 bit DAC the voltage change is 0.8 mV per step. With the stated change in frequency of 700 MHz/V from the datasheet of the radar module, this would correspond to a change in frequency of 68.8 Hz per Digital DAC step for the DIV out signal of the radar module.

The lowest change corresponds well to the measured values of the MCU as the change of the control signal changed by at most one digital bit, but the reason for the high standard deviation of the oscilloscope is unclear.

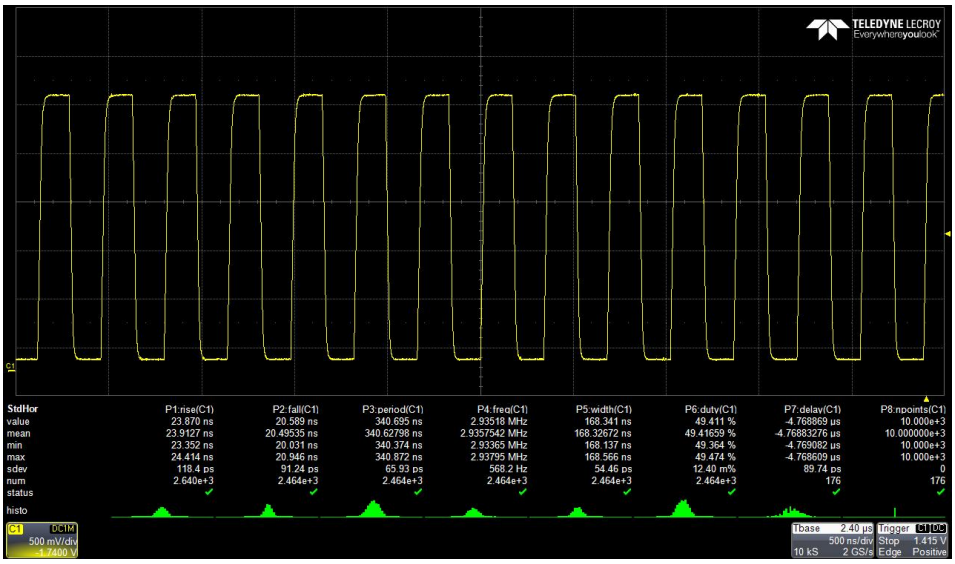

Figure 4.9: Frequency measurement - PI with static Reference value.

Due to the highly sensitive VCO the effect of ripple from the other components of the evaluation board will have a significant effect on the radar output. Therefore the PCB designed will have to be done in a way to minimise the DAC ripple. Ripple on the DAC signal could be the cause of the high standard deviation of the oscilloscope. To get better accuracy of the PI controller a higher resolution DAC could be used, for a 14 bit DAC with 3.3 V supply the voltage step size will be 200 μV. But to get any real use of this high resolution the design would have to have low ripple levels.

4.3.3 Calibration Time

The calibration time for 40 measured frequencies that are extrapolated to 200 control signals, and are used by the DAC to generate the chirp takes around 3.3 s. A PLL system can calibrate continuously between chirps or frames and this would not work with the digital control method used with the current hardware. A movement sensor radar in a security application could however get by with having delays in the lower millisecond range. With better hardware, a system of part calibrations could be used. The radar could be active for a low amount of frames, then do a small part of the calibration and then repeating the process until the full span is calibrated. By doing this over the whole control vector range, the radar would continuously update the control signals whilst minimising downtime.

The main reason for needing a re-calibration of the VCO is a temperature change. To reduce quick temperature changes, the VCO should be placed in some way so it is as protected from the elements as it can.

A simple way of increasing the calibration speed could be to use fixed point arithmetic, as computers are famously slow when doing floating point calculations. A fixed point method could improve computation speed, it does however decrease accuracy to some extent but it could be a good trade off.

The method that determines if the control value is correct uses an average error calibration in each PI update. This requires extra computation for each loop and affects the calibration time. A method that could increase the calibration speed would be to not base the correct control value on the error estimation and instead only use a set amount of time or only let the PI do a certain amount of calibration loops for each control value. By doing less computation in each loop the calibration speed could be lowered, but with the downside of losing the safety of the average error estimation.

4.3.4 Chirp Test

To evaluate the behaviour of the VCO of the Radar module, a benchmark for the non linearity was created. To do this, a program of a spectrum analyser that is specifically made for radar chirps was used. This program had several functions but the most important for the project was to be able to evaluate the slope error of the chirp.

A waveform generator was used to control the radar module and a horn antenna was connected to the spectrum analyser. The generator was set to output a sawtooth waveform with the minimum voltage and maximum voltage that correlated to an output of 24.05 GHz - 24.25 GHz and the resulting chirp of this can be seen in figure 4.10.

The program will estimate the perfect chirp depending on the measured chirp time and frequency change and it then compares this estimated "perfect" chirp to the measured chirp to get the slope error. The resulting plots of the estimated chirp and the calculated error can be seen in Figure 4.11 and 4.13. Because the waveform generator will output a linear voltage change with no adjustment to the non-linearity of the VCO the resulting chirp will be non-linear. This benchmark can then be used to evaluate the PI controlled chirp.

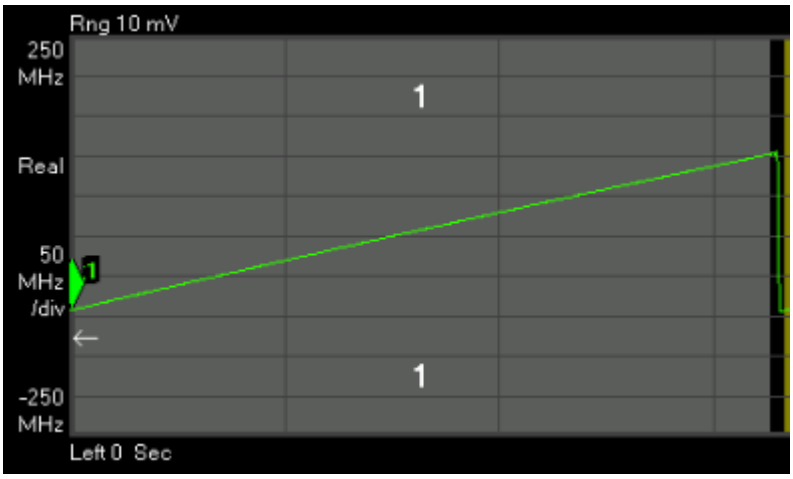

Figure 4.10: The measured chirp made from the waveform generator.

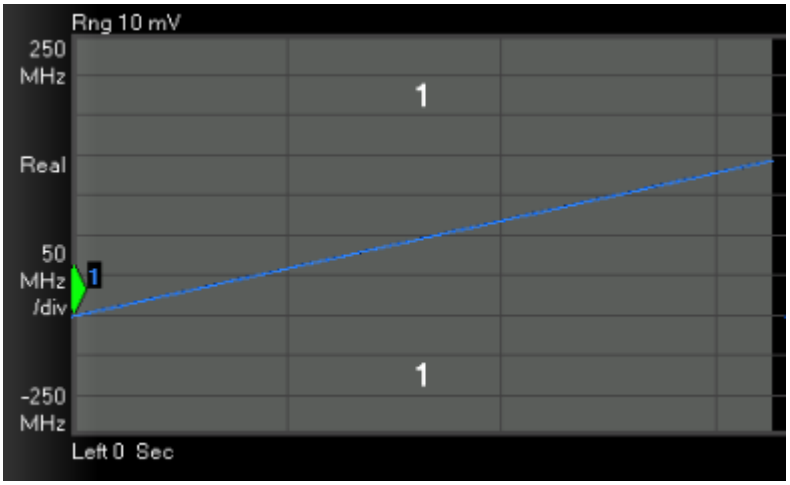

Figure 4.11: The estimated chirp, made in the spectrum analysers software.

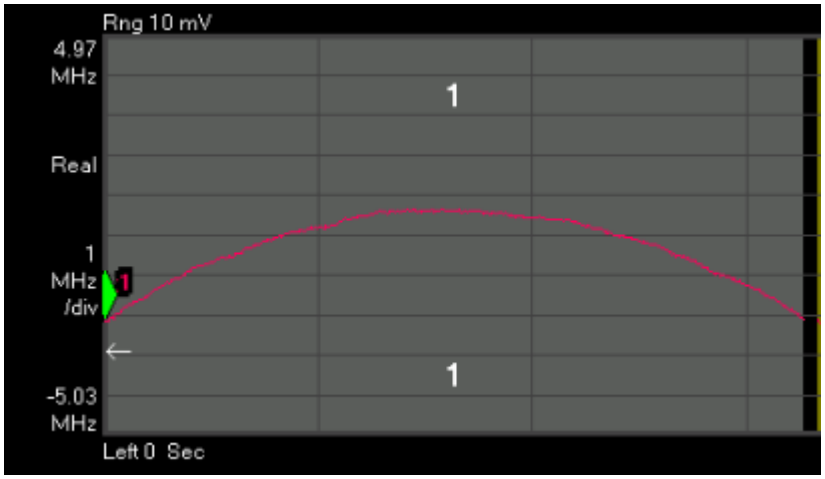

Figure 4.12: The slope error - Difference between the measured and the estimated chirp.

To evaluate the slope deviation the radar setup was tested with the same setup as for the benchmark and with the help of the results from the test, the RC filter could be optimised further to reduce the slope deviation. The chirp time was also lowered as much as the hardware could handle to increase the radar resolution.

The effect of the PI controller on the chirp linearity can be clearly seen in Figure 4.13, comparing the result and the benchmark it can be seen that the slope error of the PI controlled chirp is around 1/6 of the benchmark. The error in range measurement due to the non linearity in the benchmark can be calculated to 0.5 meters and the PI controlled system has an error of about 0.1 meters due to the remaining non linearity. This shows the method indeed does work to reduce the error caused by the non linearity of the VCO. The combined effect of the error in beat frequency, range resolution, and ADC sample rate of the beat frequency is too complicated for the scope of this master thesis.

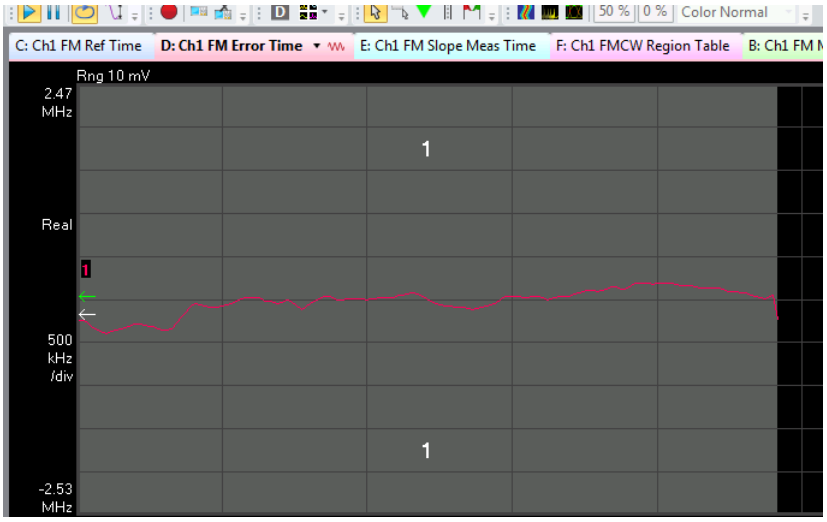

Figure 4.13: The slope error of the Calibrated chirp

Calculating the effect of the non-linearity gives an inaccuracy of about 0.5m due to the change in slope which affects the range calculation. Since the slope error is about a sixth of the benchmark on the PI controlled system, the remaining error of the slope inaccuracy will be about 0.1m.

4.3.5 Temperature Tests

To test that the calibration method can handle extreme temperatures tests were done in a climate chamber at Axis. The climate chamber can simulate temperatures in a large temperature range. The main thing to verify with this test was that even in the extreme temperatures the radar chirp frequency never left the allocated bandwidth. With the minimum and maximum measurement of an oscilloscope the frequency range could be determined. The calibration was done several times for each temperature set point to ensure that the results were consistent.

The three figures, 4.14, 4.15 and4.16, show that the minimum and maximum frequency of the measured frequency signal are close to the allowed frequency range. Some additional fine-tuning would have to be done to ensure that the chirp frequency stays inside of the allowed bandwidth.

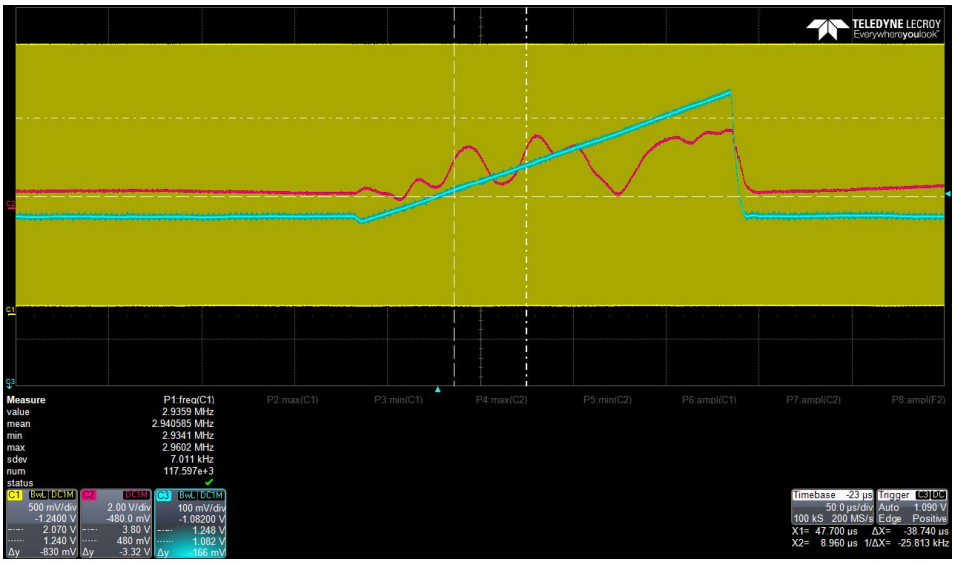

Figure 4.14: Bandwidth Test for -20C

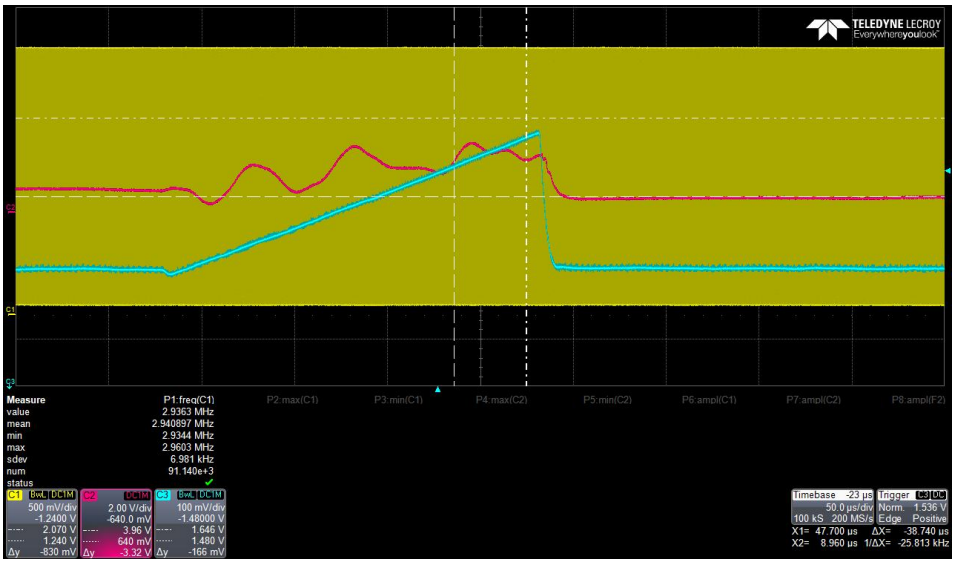

Figure 4.15: Bandwidth Test for 20C

Several calibrations were done at the same temperature and some select control values can be seen in Table 4.2, 4.3, and 4.4. This shows that while there is a small difference between each calibration, the value this amounts to could be due to the temperature not being completely stable. Another thing to note is that the Slope Error test could not be performed in a climate controlled environment due to a lack of test equipment. A strong reason for the slope error to not be as good for -20 and 40 degrees is that the total change in voltage for the chirp is different by about 15%. This will affect the voltage change between each step, which could affect the system.

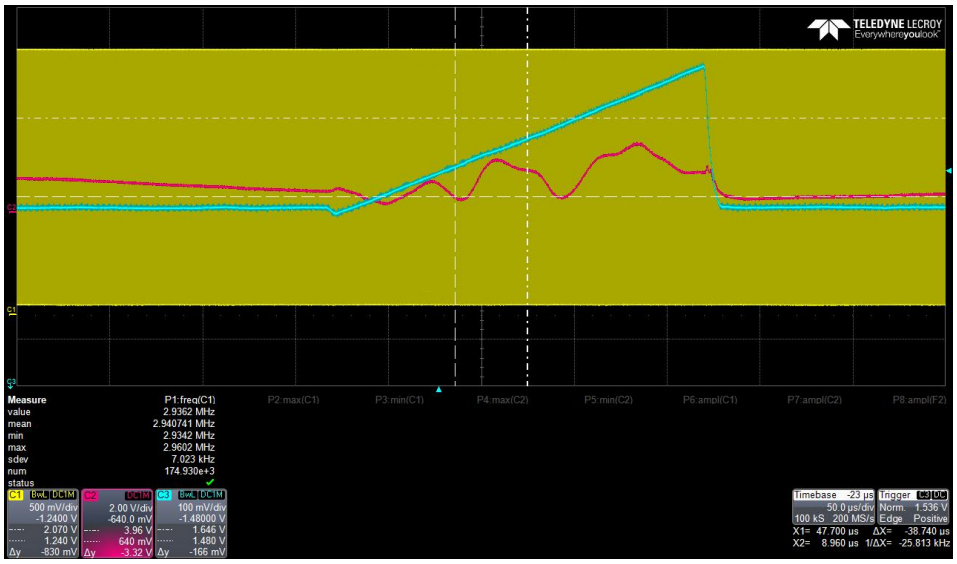

Figure 4.16: Bandwidth Test for 40C

Table 4.1: Bandwidth Test for Different Temperatures.

	Minimum frequency	Maximum frequency
Limits from ISM Band	2.9357Mhz	2.9602Mhz
-20°C	2.9341MHz	2.9602Mhz
23°C	2.9341Mhz	2.9602MHz
40°C	2.9342MHz	2.906MHz

4.4 IQ signals & ADC

To ensure the functionality of the radar with this control method some tests where done on the IQ signals. These signals are the ones that will contain the beat frequency. The sampling and stability of these signals are therefore important.

4.4.1 DAC

The RC filter and the change in voltage for each step of the DAC are two things that are closely connected due to how the capacitor gets charged. Several different step sizes were tested for the DAC, but with each step size the RC filter has to be recalibrated which takes a lot of time. A low amount of steps allows for a quicker chirp, but there are several drawbacks in using a low amount of steps. The most obvious is that the non-linearity is harder to control. The relatively long time between steps required a large capacitance to linearity the digital steps. This capacitance can cause problems when sending several consecutive chirps. A larger capacitor takes longer time to discharge and the radar can not start the next chirp until the voltage is down to idle level before starting the next chirp if the full bandwidth is to be used. Therefore the step size was set to as small as possible while still having a high enough maximum velocity required for the application.

Table 4.2: Control Values for -20° C.

	Calibration 1	Calibration 2	Calibration 3
Control Value [0]	1317	1319	1322
Control Value [100]	1494	1495	1499
Control Value [200]	1675	1678	1680
Total Change	358	359	358

Table 4.3: Control Values for 23° C.

	Calibration 1	Calibration 2	Calibration 3
Control Value [0]	1681	1682	1683
Control Value [100]	1877	1877	1879
Control Value [200]	2079	2079	2079
Total Change	398	397	396

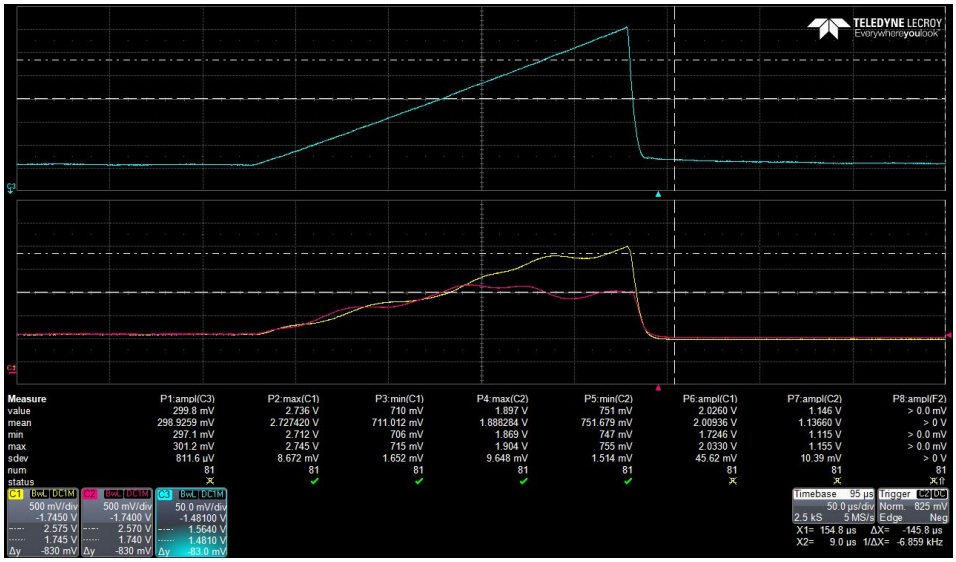

Figure 4.17: Chirp with RC filter on the top plot with IQ signals on the Bottom.

Amplification of IQ signals

The raw IQ signal had a max voltage range of about 100 mV from its lowest to its highest level. With the 12 bit ADC with a supply voltage of 3.3 V it would result in step sizes of $3.3/2^{12}$ volts. This, in turn gives the raw signal a digital span of 124 digital steps. The 100 mV change over 80 ADC measurements is noticeable, however, as can be seen in Figure 4.21 the data is too noisy to get any real results. With the active band-pass filter with a gain of 20, a lower bound of 100 Hz and an upper limit of 100 kHz, the ADC measurement was significantly improved while still retaining the important information of the signal. This can be seen in Figure 4.20. Both of these

Table 4.4: Control Values for 40° C.

	Calibration 1	Calibration 2	Calibration 3
Control Value [0]	1840	1842	1839
Control Value [100]	2045	2047	2045
Control Value [200]	2255	2258	2256
Total Change	415	416	417

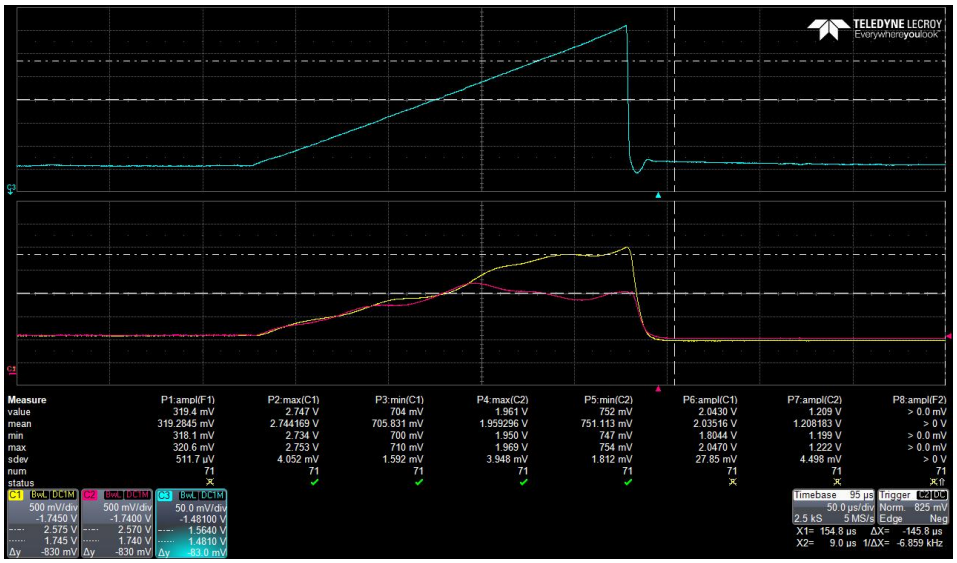

Figure 4.18: Chirp with no RC filter on the top plot with IQ signals on the Bottom.

pictures show the ADC data extracted from the MCU. Since the gain is set to 20 the resulting signal has a peak to peak of around 2 volts which equates to digital span of around 2400.

As can be seen in Figure 4.19 which shows both the I and Q signals with the amplified signal and the raw signal overlaid, the amplified signal follows the raw signal closely with little distortion due to the operational amplifier. There is however some distortion at the end of the chirps, this shows that the amplifier can handle the current rate of change but it has to be evaluated more closely to ensure the correct function.

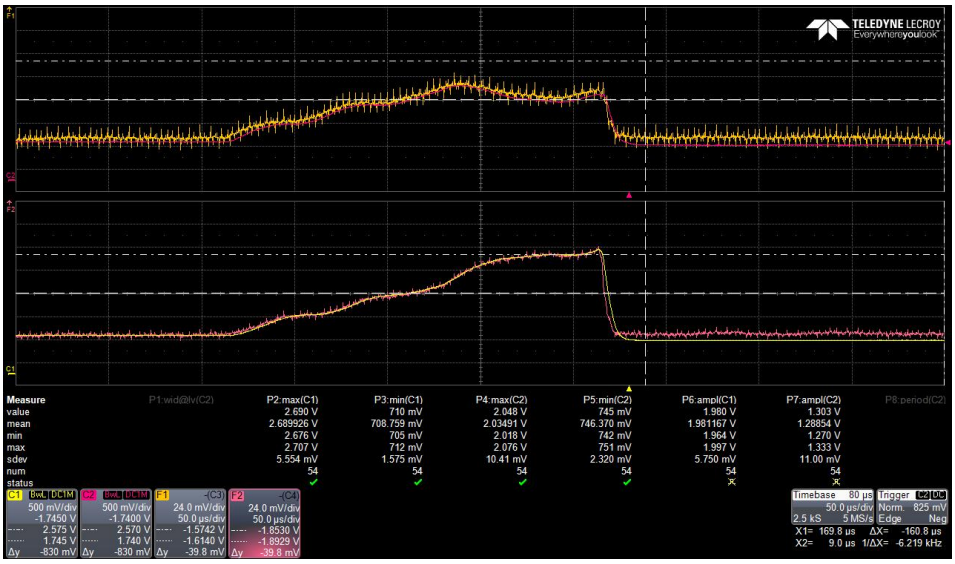

Figure 4.19: IF-signal with both the amplified and raw signal. Top I and Bottom Q.

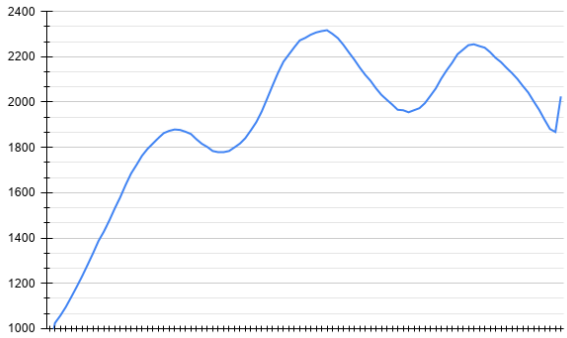

Figure 4.20: ADC data from amplified signal.

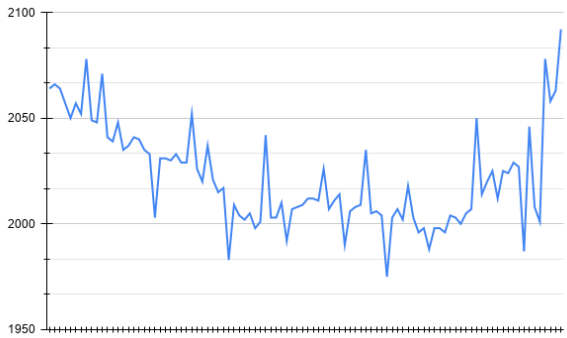

Figure 4.21: ADC data from raw signal.

Stability of IQ signals

To ensure stability of both of the IQ signals the oscilloscope was set to continuously save the plots and overlay them on the grid as can be seen in Figure 4.22. When there is no movement around the radar it can be seen that there are no sudden irregularities caused by the hardware or the code that could trigger a false positive.

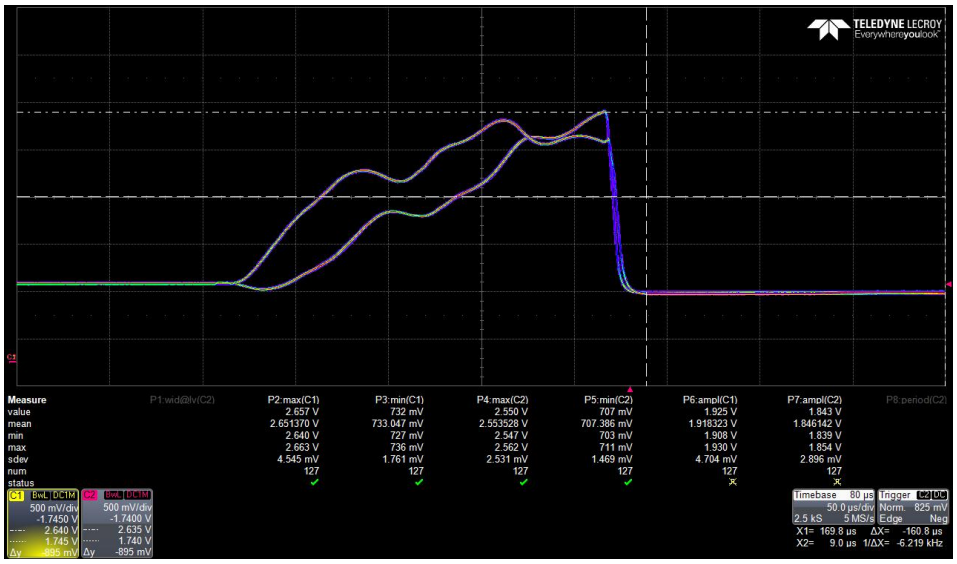

Figure 4.22: Persistence test of radar.

4.4.2 Range Measurement

A range measurement test against a wall was performed to evaluate the beat frequency, with an oscilloscope, pictures of the waveform could be taken at a distance of 3, 5, 7 and 10 meters. The data of the pictures were then analysed in two ways to calculate the range to the target wall. Firstly by measuring the time between two peaks of the image to get the beat frequency and then applying the range formula. With the pictures from the oscilloscope the data points were saved, this data could then be analysed with Octave. Octave which is a high level programming language that is commonly used for mathematical computations, has functions for doing Fast Fourier Transforms. A FFT plot was created of the beat frequency and the peaks of the plot could then be used to extract range information.

During the range measurement test, a clear change in beat frequency can be seen in Figure 4.23, 4.24, 4.25 and 4.26, depending on the range to the wall. But when trying to detect a human that walks past the radar the signal strength was too low to see directly on the oscilloscope. Using Range FFT over several chirps could in theory improve the signal strength and perhaps detect a target better. 10 meter range is stated in the datasheet so this could be possible.

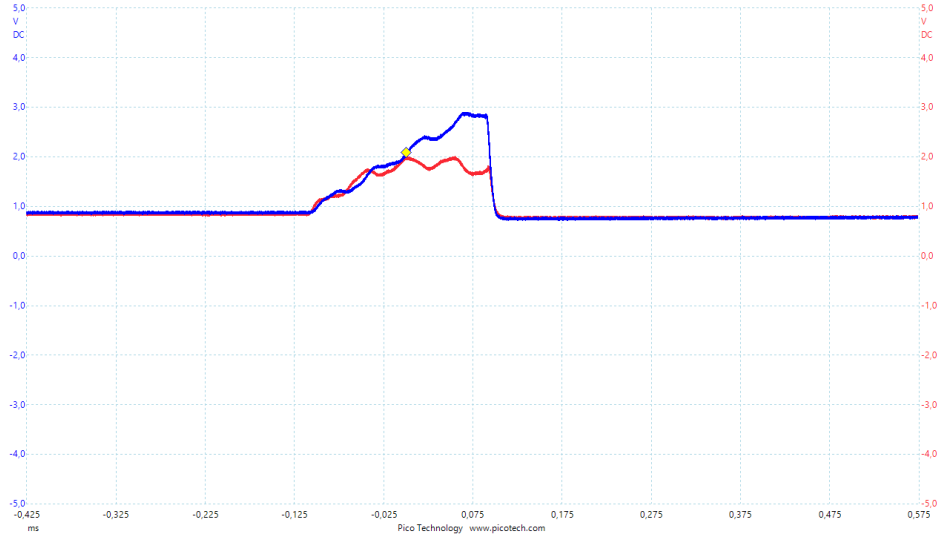

Figure 4.23: IF signal test 3 Meters

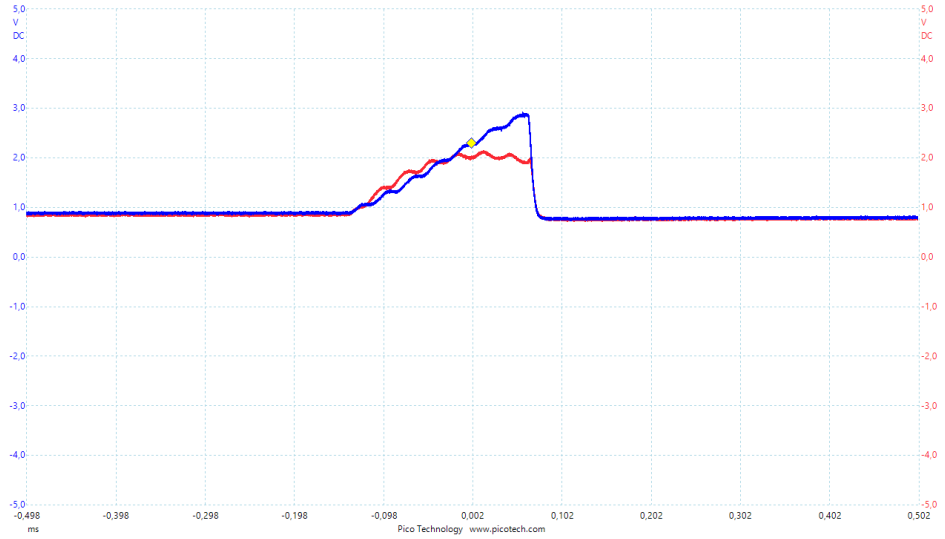

Figure 4.24: IF signal test 5 Meters

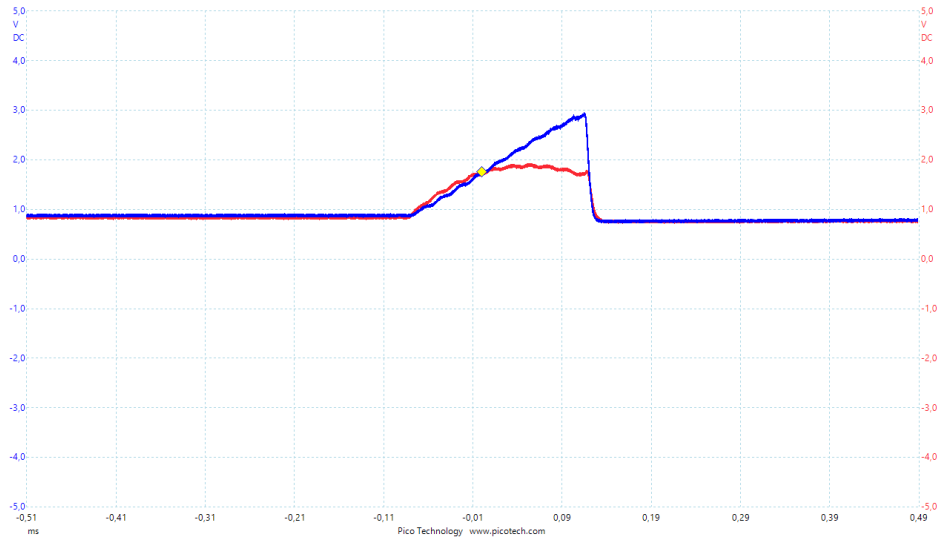

Figure 4.25: IF signal test 7 Meters

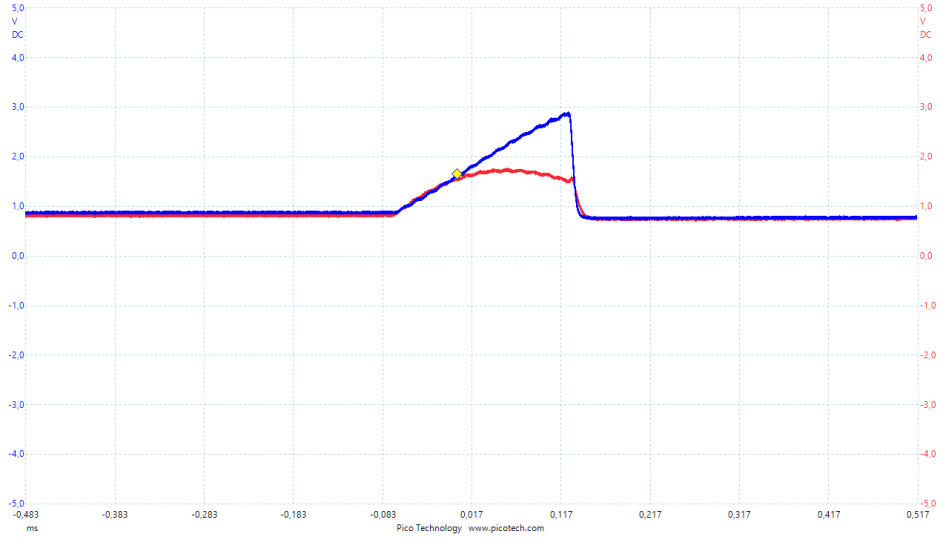

Figure 4.26: IF signal test 10 Meters

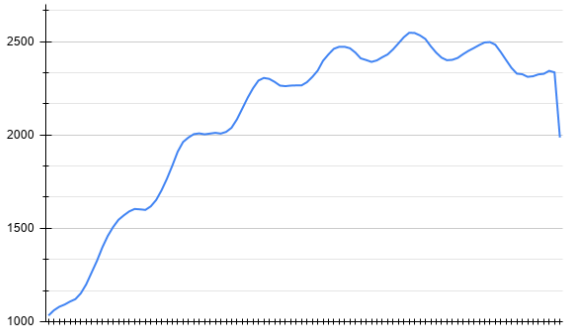

Figure 4.27: ADC data for I signal of 5 meter for comparison

4.4.3 FFT test

Some basic FFT tests with Octave were done on the data collected from the ADC conversion of the range measurements and the plots of these tests can be seen in Figure 4.28, 4.29, 4.30, and 4.31. The peak in the plots that correlates to the beat frequency can be seen, but it is not particularly clear if the correct beat frequency is known. The effects of the cross talk can also be seen clearly in the low frequencies. These plots show the necessity of using FFT over several chirps as was described in the theory part of the thesis.

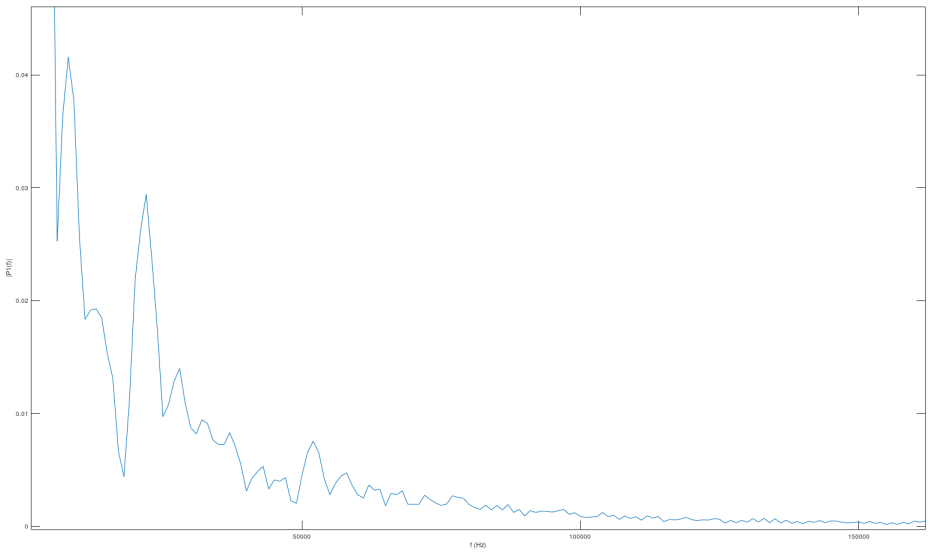

Figure 4.28: FFT of I signal 3 meter

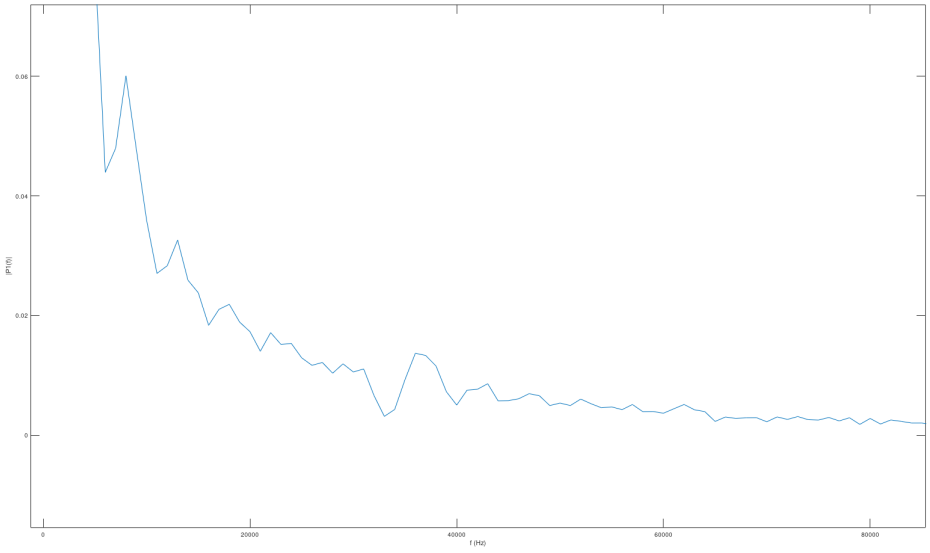

Figure 4.29: FFT of I signal 5 meter

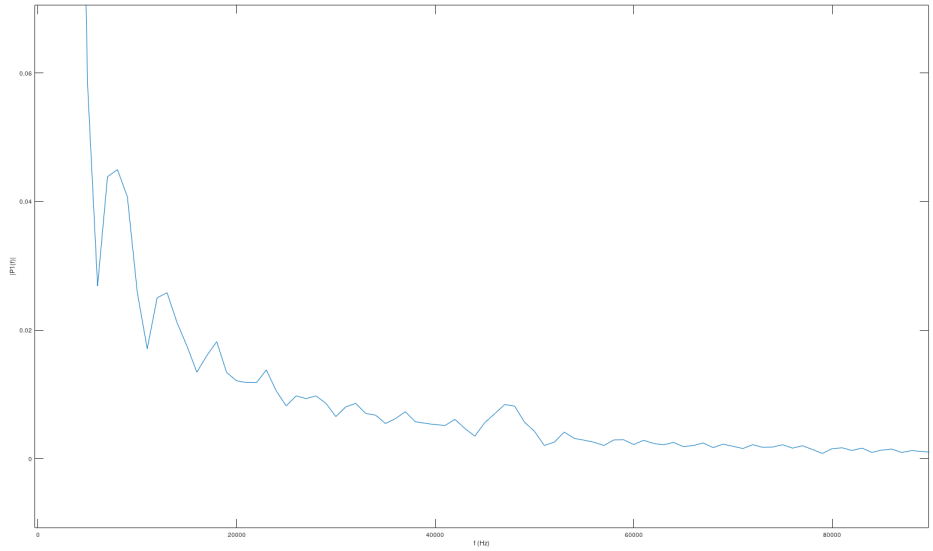

Figure 4.30: FFT of I signal 7 meter

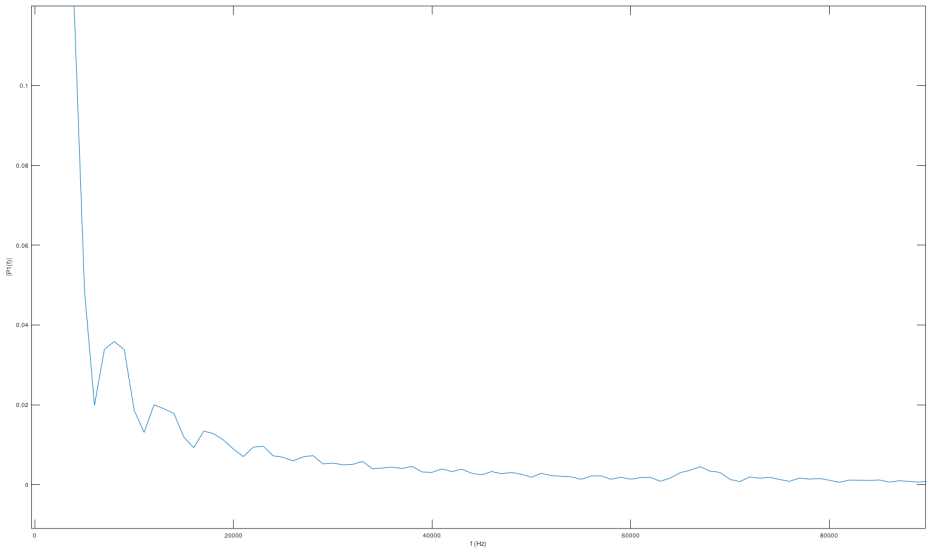

Figure 4.31: FFT of I signal 10 meter

4.5 Improvements and Further Development

In this chapter possible improvements for the current solution will be presented. The improvements mainly have to do with the hardware and IF signal analysis.

The ADC of the STMF401RB only has one channel, this causes a delay of one ADC sampling between each conversion when sampling two different channels. This is not ideal when using two antennas to acquire angle data of the target. If both I and Q data is wanted for two antennas there would have to be 4 ADC channels to ensure that all of the measurements are done in sync.

A radar with only one RX antenna and IQ modulation, as the SMR-334 has, can only measure movement, velocity, and the direction of the target. But it cannot measure the angle of arrival to the target. Depending on the use case of the radar this could be an important data point. In theory the resolution of two RX is still quite low, but each channel that has to be sampled requires an additional ADC channel to be able to have good accuracy.

Innosent, the creator of the radar module also has explanations of another way to measure velocity of a target. Instead of measuring the phase shift between the chirps the Doppler frequency change can be measured. For a final product, both of these methods should be evaluated, so that the best method can be used.

5 Conclusion

This thesis has shown the performance of a mid range MCU being used as a PI controller for a VCO and how it can be used to reduce the inherent problems with the VCO's non-linearity and temperature dependency.

The system works as intended and it limits the VCO non-linearity to a large degree, it has also been shown to be able to contain the frequency modulated signal close to the allowed bandwidth and by setting a slightly larger error margin it can be contained completely within the allowed bandwidth.

The hardware chosen for the project had to be pushed to the edge of what it was capable both to measure frequency and to calibrate the control signal. To use this type of system in a product a slightly better MCU with higher clock frequency could improve both the control loop and the signal analysis. Further development with an MCU with a larger memory but the same system layout should be able to work as a movement sensor for security applications. The main problem with the system is the extra calibration time that comes with the use of a PI controller instead of PLL, this problem could however be reduced to a level where the downtime associated with the calibration can be lowered to the point where it is no longer a large issue.

As MCUs get faster and cheaper this control method may be viable for a retail product, but things like lowered calibration time and the need of several ADC channels to sample several receiving channels have to be implemented for a good final product.

Bibliography

[1] Dario Tarchi, Michele Vespe, Ciro Gioia, Francesco Sermi, Vladimir Kyovtorov and Giorgio Guglieri. "Low-Cost Mini Radar: Design Prototyping and Tests". In: *Journal of Sensors* 2017 (July 2017), pp. 1–15. DOI: 10.1155/2017/8029364.

[2] *Frequency ranges for automotive radar technology.* URL: https://www.cetecom.com/en/news/frequency-ranges-for-automotive-radar-technology/. (accessed: 25.05.2021).

[3] Sang Gi Hong, Nae Soo Kim and Whan Woo Kim. "Reduction of False Alarm Signals for PIR Sensor in Realistic Outdoor Surveillance". In: *ETRI Journal* 35.1 (2013), pp. 80–88. DOI: https://doi.org/10.4218/etrij.13.0112.0219. eprint: https://onlinelibrary.wiley.com/doi/pdf/10.4218/etrij.13.0112.0219. URL: https://onlinelibrary.wiley.com/doi/abs/10.4218/etrij.13.0112.0219.

[4] Merrill I. Skolnik. "History Of Radar Early experiments". In: (). URL: https://www.britannica.com/technology/radar/History-of-radar.

[5] National Research Council. "Role of Radar in the Weather and Climate Observing and Predicting System". In: (2002). URL: https://www.nap.edu/read/10394/chapter/3.

[6] *What is the Difference Between FrequencyModulated Continuous-Wave (FMCW) and Pulsed Wave or Pulsed Width Radar?* URL: https://www.automation.com/getattachment/d201a032-1c4b-4885-b41b-b2c0400b3cd2/FMCW-vs-Pulse-Radar-White-Paper.pdf?lang=en-US&ext=.pdf. (accessed: 25.05.2021).

[7] *What is the C Band?* URL: https://www.everythingrf.com/community/c-band. (accessed: 25.05.2021).

[8] *What is the X-Band?* URL: https://www.everythingrf.com/community/x-band. (accessed: 25.05.2021).

[9] *What is the K Band?* URL: https://www.everythingrf.com/community/k-band. (accessed: 25.05.2021).

[10] *What is the W Band?* URL: https://www.everythingrf.com/community/w-band. (accessed: 25.05.2021).

[11] *ISM Bands.* URL: https://siliconradar.com/wiki/ISM_Bands. (accessed: 25.05.2021).

[12] Wolfgang Weidmann. "APPLICATION NOTE I". In: (). URL: https://www.innosent.de/fileadmin/media/dokumente/Downloads/Application_Note_I_-_web.pdf.

[13] European Space Agency. *File:Diagram defining parameters for radar equation.jpg.* URL: https://en.citizendium.org/wiki/File:Diagram_defining_parameters_for_radar_equation.jpg. (accessed: 25.05.2021).

[14] Christian Wolff. *Directivity and Antenna Gain*. URL: https://www.radartutorial.eu/06.antennas/an07.en.html. (accessed: 25.05.2021).

[15] Henrik Forstén. *Third version of homemade 6 GHz FMCW radar*. URL: https://hforsten.com/third-version-of-homemade-6-ghz-fmcw-radar.html. (accessed: 25.05.2021).

[16] S. Suleymanov. *Design and Implementation of an FMCW Radar Signal Processing Module for Automotive Applications*. 2016. URL: http://essay.utwente.nl/70986/.

[17] Christian Wolff. *Frequency-Modulated Continuous-Wave Radar (FMCW Radar)*. URL: http://www.radartutorial.eu/02.basics/FrequencyModulatedContinuousWaveRadar.en.html. (accessed: 25.05.2021).

[18] Jan Luca Uphoff. "Introduction to automotive FMCW Radar Technologies: Using Texas Instruments mmWave AWR sensor series". In: (). URL: http://urn.kb.se/resolve?urn=urn:nbn:se:bth-16266.

[19] Christian Wolff. *Range Resolution*. URL: https://www.radartutorial.eu/01.basics/Range%20Resolution.en.html. (accessed: 25.05.2021).

[20] Sandeep Rao. "Introduction to mmwave Sensing: FMCW Radars". In: (). URL: https://training.ti.com/sites/default/files/docs/mmwaveSensing-FMCW-offlineviewing_4.pdf.

[21] Jessica Nilsson and Ludvig Hassbring. *Machine Learning for FMCW Radar Interference Mitigation*. eng. Student Paper. 2020.

[22] M. Schüssel. "Angle of Arrival Estimation using WiFi and Smartphones". In: 2016.

[23] Christian Wolff. *IQ radar*. URL: https://www.radartutorial.eu/10.processing/sp06.en.html. (accessed: 25.05.2021).

[24] Infineon. *MakeRadar School - Radar Theory*. URL: https://www.infineon.com/cms/en/product/promopages/makeradar/makeradar-school/radar-theory/.

[25] Wolfgang Weidmann. *APPLICATION NOTE II*. URL: https://www.innosent.de/fileadmin/media/dokumente/Downloads/Application_Note_II_-_web.pdf.

[26] Janusz S. Kulpa. "Noise radar sidelobe suppression algorithm using mismatched filter approach". In: *International Journal of Microwave and Wireless Technologies* 8.6 (2016), 865–869. DOI: 10.1017/S1759078716000945.

[27] Guoying Wu, Kexu Sun, Shita Guo, Tao Zhang, Tianzuo Xi, Rui Wang and Ping Gui. "A low-voltage and temperature compensated ring VCO design". In: Oct. 2014, pp. 1–4. DOI: 10.1109/DCAS.2014.6965321.

[28] Wang Hua, Song Qian and Zhou Zhi-min. "Nonlinearity estimation and correction of VCO based on temperature-varied tuning characteristic model". In: *2013 Asia-Pacific Microwave Conference Proceedings (APMC)*. 2013, pp. 797–799. DOI: 10.1109/APMC.2013.6694935.

[29] Shuo Jiang, Bo Liu, Huachuang Wang and Bin Zhao. "Absolute Distance Measurement Using Frequency-Scanning Interferometry Based on Hilbert Phase Subdivision". In: *Sensors* 19.23 (2019). ISSN: 1424-8220. DOI: 10.3390/s19235132. URL: https://www.mdpi.com/1424-8220/19/23/5132.

[30] *Integrated Phase-Locked Loops Offer Higher-Frequency Performance, Enhanced User Benefits*. URL: https://www.digikey.se/sv/articles/integrated-phase-locked-loops-offer-higher-frequency-performance-enhanced-user-benefits.

[31] Martina Maggio. *Approximation of Analog Controllers, PID Control*. Feb. 2020. URL: https://www.control.lth.se/fileadmin/control/Education/EngineeringProgram/FRTN01/lectures/L08_slides6.pdf.

[32] InnoSent. *User Manual SMR-314/334*. Aug. 2020.

[33] Manas Sharma. *Polynomial Fitting – C PROGRAM*. URL: https://www.bragitoff.com/2018/06/polynomial-fitting-c-program/.

[34] STMicroelectronics. *STM32 Nucleo-64 development board with STM32F410RB MCU, supports Arduino and ST morpho connectivity*. URL: https://www.st.com/en/evaluation-tools/nucleo-f410rb.html.

A Appendix

Some closer pictures of the prototype

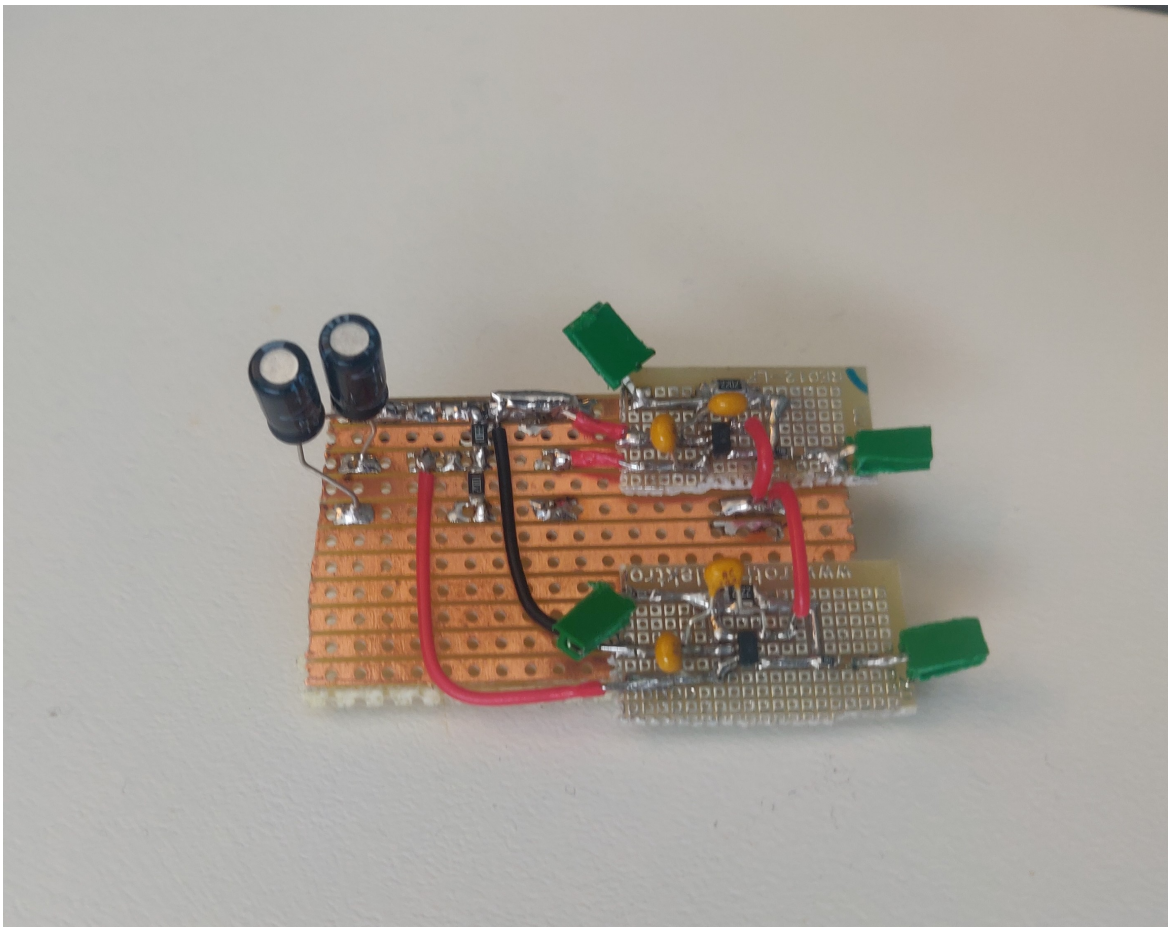

Figure A.1: Active band pass filter

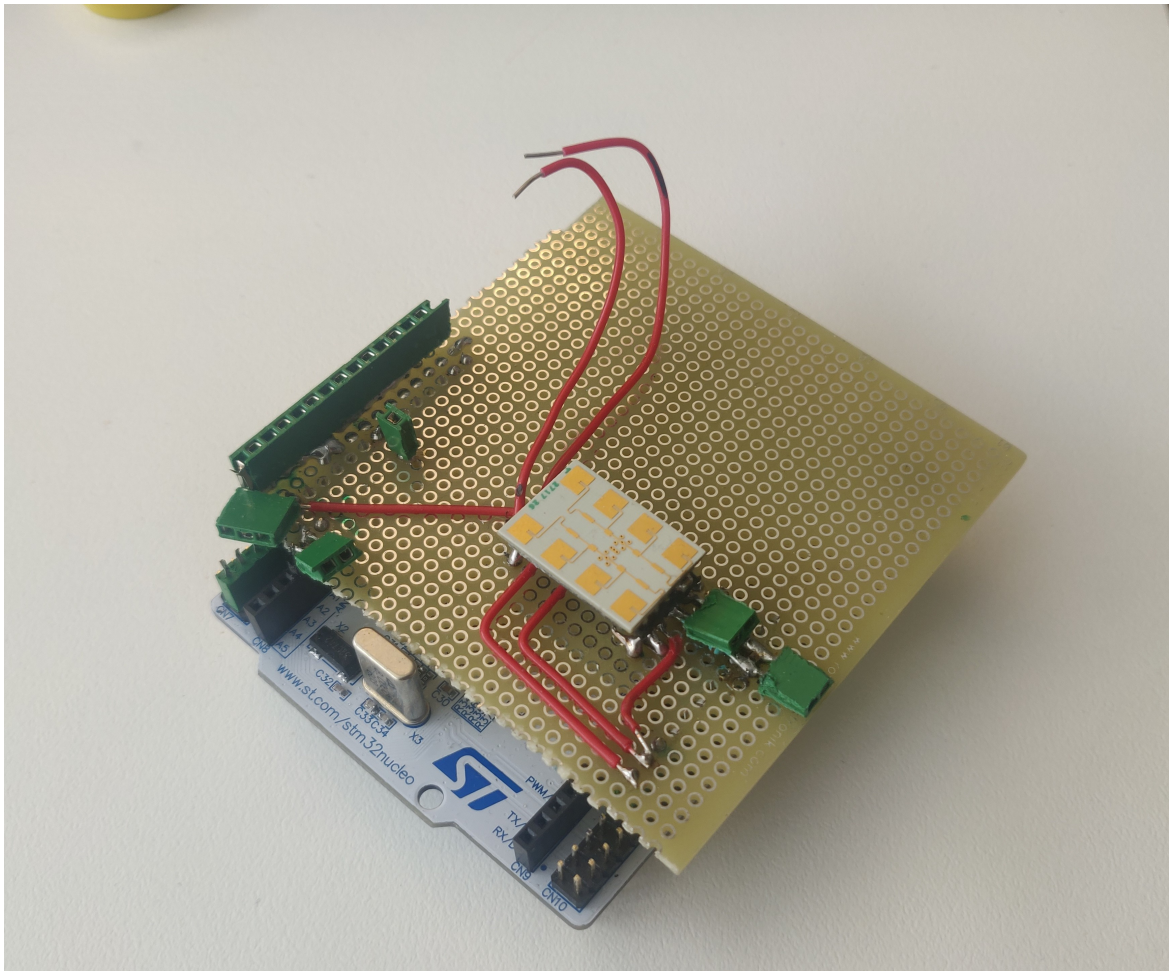

Figure A.2: Evaluation board with radar module and RC-filter

Lund University
Department of Automatic Control
Box 118
SE-221 00 Lund Sweden

Document name
MASTER'S THESIS

Date of issue
August 2021

Document Number
TFRT-6148

Author(s)
Martin Alumets
Mattias Evaldsson

Supervisor
Lars Andersson, AXIS, Sweden
Andreas Glatz, AXIS, Sweden
Anton Cervin, Dept. of Automatic Control, Lund University, Sweden
Kristian Soltesz, Dept. of Automatic Control, Lund University, Sweden (examiner)

Title and subtitle
Digital Control of a VCO for Radar Applications

Abstract

Radar systems have been around since the early 20th century, and technology is advancing at an ever-increasing speed. This has led to great achievements in radar development, which have expanded the technology's area of use. One of these is the application of a security radar used in conjunction with security cameras for increased flexibility and reliability in security systems. A type of radar that is suited for security applications is the frequency modulated continuous wave radar, and it requires a control system to stay within the allocated radar frequency spectrum and to increase the radar's performance. This control system is often implemented with analogue components, which comes with extra costs and space requirements. This master thesis aims to investigate a digital control method and analyse the performance of it. This comes with the advantage of not requiring any extra components for the control system and rely on the micro control unit used to analyse the radar data.

Keywords

Classification system and/or index terms (if any)

Supplementary bibliographical information

ISSN and key title
0280-5316

ISBN

Language
English

Number of pages
1-66

Recipient's notes

Security classification